Available online at www.sciencedirect.com
ScienceDirect
Marine and Petroleum Geology 26 (2009) 57–84
Marine and Petroleum Geology
www.elsevier.com/locate/marpetgeo

Depositional environment and hydrocarbon source potential of the Oligocene Ruslar Formation (Kamchia Depression; Western Black Sea)

R.F. Sachsenhofer[a,*], B. Stummer[a], G. Georgiev[b], R. Dellmour[c], A. Bechtel[a,d], R. Gratzer[a], S. Corić[e]

[a]*Department of Applied Geosciences and Geophysics, Montanuniversität Leoben, Peter-Tunner-Str. 5, A-8700 Leoben, Austria*
[b]*Department of Geology and Paleontology, Sofia University "St. Kliment Ochridski", 15 Tsar Osvoboditel Blvd., 1504 Sofia, Bulgaria*
[c]*OMV Exploration & Production, GmbH/OMV, Bulgaria Offshore Exploration, Gerasdorfer Straße 151, A-1210 Vienna, Austria*
[d]*Mineralogisch-Petrologisches Institut, Universität Bonn, Poppelsdorfer Schloss, D-53115 Bonn, Germany*
[e]*Geological Survey of Austria, Neulinggasse 38, A-1030 Vienna, Austria*

Received 17 January 2007; received in revised form 16 August 2007; accepted 19 August 2007

Abstract

The Oligocene Ruslar Formation is a hydrocarbon source rock in the Kamchia Depression, located in the Western Black Sea area. Depositional environment and source potential of the predominantly pelitic rocks were investigated using core and cuttings samples from four offshore wells. In these wells the Ruslar Formation is up to 500 m thick. Based on lithology and well logs, the Ruslar Formation is subdivided from base to top into units I–VI. Dysoxic to anoxic conditions and mesohaline to euhaline salinities prevailed during deposition of the Ruslar Formation. Relatively high oxygen contents occurred during early Solenovian times (lower part of unit II), when brackish surface water favoured nannoplankton blooms and the deposition of bright marls ("Solenovian event"). Anoxic conditions with photic zone anoxia were established during late Oligocene times (units III and IV) and, probably, reflect a basin-wide anoxic event in the Eastern Paratethys during Kalmykian times. Organic carbon content in the Ruslar Formation is up to 3%. Autochthonous aquatic and allochthonous terrigenous biomass contribute to the organic matter. Relatively high amounts of aquatic organic matter occur in the lower part of the Ruslar Formation (units I and II) and in its upper part (unit VI). Diatoms are especially abundant in the lower part of unit VI. The kerogen is of type III and II with HI values ranging from 50 to 400 mgHC/gTOC. Units I and II (Pshekian, lower Solenovian) are characterized by a fair (to good) potential to produce gas and oil, but potential sources for gas and oil also occur in the Upper Oligocene units IV–VI.

Keywords: Paratethys; Oligocene; Black Sea; Bulgaria; Ruslar Formation; Source rock; Organic matter

1. Introduction

Organic-rich rocks were deposited during Oligocene times in the Paratethys, a marginal sea which formed after the Eocene break-up of the Tethys (e.g. Vetö, 1987; Popov et al., 2004; Kotarba and Koltun, 2006; Sachsenhofer and Schulz, 2006; Fig. 1a). Within the Eastern Paratethys, the pelitic Oligocene and Lower Miocene rocks are generally known as Maykop Shale. In the Kamchia Depression (onshore and offshore Bulgaria; Western Black Sea; Fig. 1b), the term Ruslar Formation is used for the Oligocene succession (e.g. Aladžova-Hrisčeva, 1991; Fig. 2).

Although considered potential source rocks, relatively few data on the source potential of the Maykop Shale are available in literature. Moreover, most of these papers focus on the South Caspian Basin (e.g. Abrams and Narimanov, 1996; Katz et al., 2000) and the Caucasus area (e.g. Saint-Germès et al., 2000, 2002), whereas data from the Black Sea area and the Ruslar Formation are scanty (e.g. Trotsuk et al., 1993; Georgiev, G.V., 1996, 2004; Fadeeva and Bazhenova, 2003; Bazhenova et al., 2003).

*Corresponding author. Tel.: +43 3842 402 6104; fax: +43 3842 402 6102.
E-mail address: Reinhard.Sachsenhofer@mu-leoben.at (R.F. Sachsenhofer).

0264-8172/$ - see front matter © 2007 Elsevier Ltd. All rights reserved.
doi:10.1016/j.marpetgeo.2007.08.004

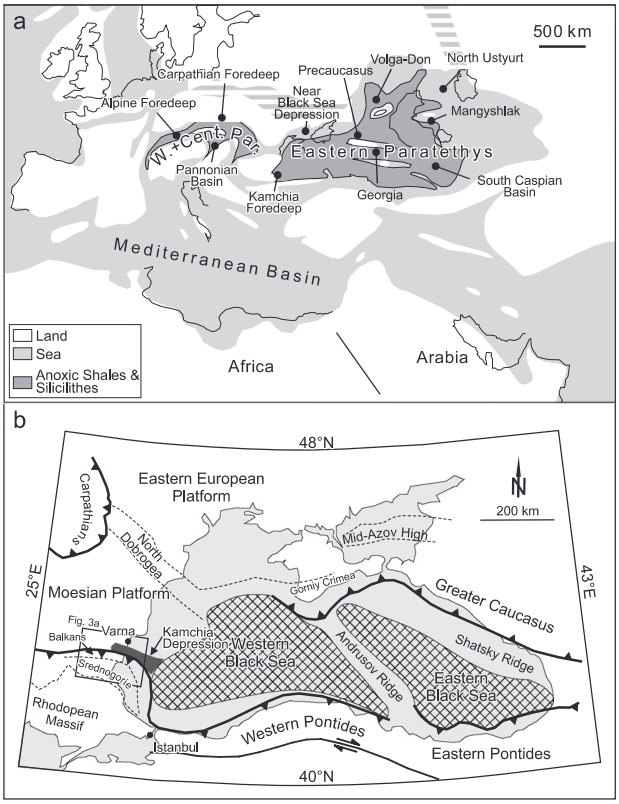

Fig. 1. (a) Paleogeographic map of the Paratethys during Early Oligocene time (simplified after Popov et al., 2004) and (b) tectonic elements of the Black Sea area (after Spadini et al., 1997). W.+C. Par. = Western and Central Paratethys.

Therefore, the main aim of the present paper was to study the lithology, depositional environment, and hydrocarbon potential of the Oligocene succession and to explore vertical and lateral facies variations. To reach this goal, material from the Ruslar Formation of boreholes LA-IV-3, Samotino More, Samotino Iztok, and LA-IV-2 (see Fig. 3a for location of wells) was studied using calcareous nannoplankton, bulk geochemical parameters (inorganic and organic carbon, total sulphur, hydrogen index), biomarker distribution, and stable carbon isotope composition of organic matter and calcite. Only three relatively short cores were taken in the wells. Therefore, the study is based on the cores and on cuttings samples.

2. Geological setting

Loading of the Moesian Platform by the Balkan thrust sheets resulted in the formation of the Paleogene Kamchia Foredeep (Figs. 3a and b; Robinson et al., 1996), which became the deep western branch of Western Black Sea Basin during mid-Eocene times (Georgiev, G., 2000, 2004). A comprehensive overview on the development of the Balkans and the Kamchia Foredeep is given by Sinclair et al. (1997), who emphasize the close relation between the Cainozoic basin fill and the shortening across the Balkans during early Paleocene to late Oligocene times. The following description follows these authors. At end Cretaceous/early Tertiary times, the northern part of the Kamchia Foredeep was characterized by emergence, whereas calci-turbidites accumulated in its deep southern part near the evolving Balkan Orogen. During early Eocene times the northern margin of the Kamchia Foredeep experienced a transgression, and siliciclastics were deposited in the south and the center of the basin. Middle Eocene and younger rocks overlie the Lower Eocene rocks with an angular unconformity (“Illyrian Unconformity”-Lutetian). A middle Eocene deepening of the northern part of the basin is related with subsidence in

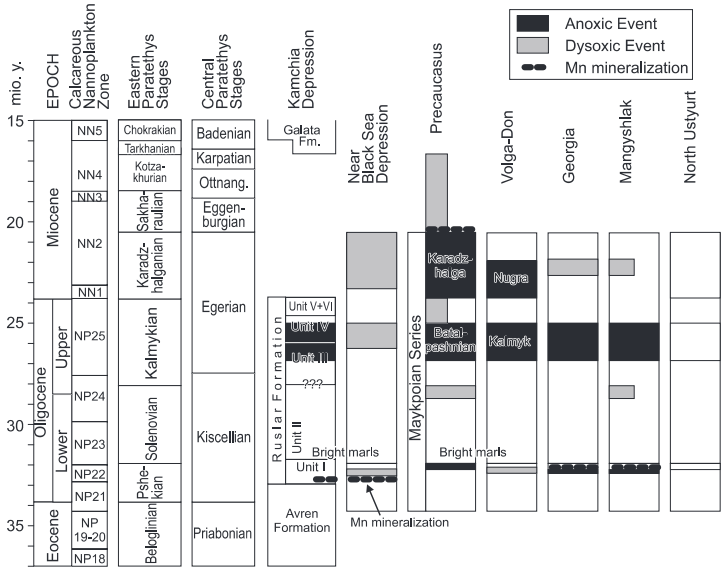

Fig. 2. Stratigraphic columns for different parts of the Eastern Paratethys (simplified after Popov and Stolyarov, 1996; see Fig. 1a for location). The time-scale follows Popov et al. (2004). The stratigraphy of the Kamchia Depression has been added after Popov and Kojumdjieva (1987), Aladžova-Hriščeva (1991) and considering new data obtained within the present study. These include nannoplankton data and the stratigraphic position of an anoxic event in the Ruslar Formation.

the Western Black Sea Basin and resulted in the accumulation of the Avren Formation (Middle to Upper Eocene), up to 1.5 km thick. It is composed of sandy marls with limestone and sandstone intercalations.

The overlying Oligocene Ruslar Formation is made up predominantly of finely laminated pelitic rocks with rare sandstones, siltstones and limestone beds representing outer shelf to shoreface facies. A major manganese mineralization occurs in the lower part of the Ruslar Formation (NP22) and is exploited in the Varna mining district (Aleksiev and Bogdanova, 1974). The mineralized horizon includes tuffitic layers and is overlain by a "clayey-silty-limy" interval with grey, dense carbonaceous clays. In the Varna area the upper part of the Ruslar Formation is dominated by laminated clays ("clayey horizon"). The thickness of the Ruslar Formation varies considerably from 60 to 70 m in the Varna area to 500 m in the shelf sector of the Kamchia Basin (e.g. Samotino More) to over 1500 m in the deep offshore of the Western Black Sea basin. Prominent erosional features within the Ruslar Formation are visible in offshore seismic lines (Fig. 3c). These erosional events were triggered by the uplifting of the Balkanides and are related to the development of a W–E trending channel belt in the Kamchia branch of the Western Black Sea Basin. Another major erosional unconformity separates the Ruslar Formation from the overlying Middle Miocene Galata Formation (Popov and Kojumdjieva, 1987; Marinov, 1997). Seismic lines from the north-western shelf of the Black Sea (Tiapkina, 2006) show similar erosional features suggesting that erosion was a widespread phenomenon in the nearshore area along the Western Black Sea shelf during Oligocene–Early Miocene times.

The Galata Formation is dominated by sands, intercalated by frequent clay and rare limestone beds (Popov and Kojumdjieva, 1987). The outcrops in the area south of Varna along the coast represent a shallow marine environment with a predominantly sandy facies of beach sands, tidal deposits and deltaic channels with occasional interdistributary fluvial to lagoonal deposits (Ori, 2004) rich in land plants. Dark grey to black shales from these interdistributary deposits yielded a rich flora of well-preserved pollen and spores as well as poor preserved calcareous nannoplankton indicating Middle to Upper Miocene age (Ćorić and Zetter, 2004).

The shallow offshore well Samotino More tested gas and minor condensate from siliciclastic intervals in the Avren Formation of Middle Eocene age.

3. Material and methods

Samotino More, drilled in 1985/86, was selected as a key well, because it is the only one with cuttings samples representing the entire Ruslar Formation, and because it

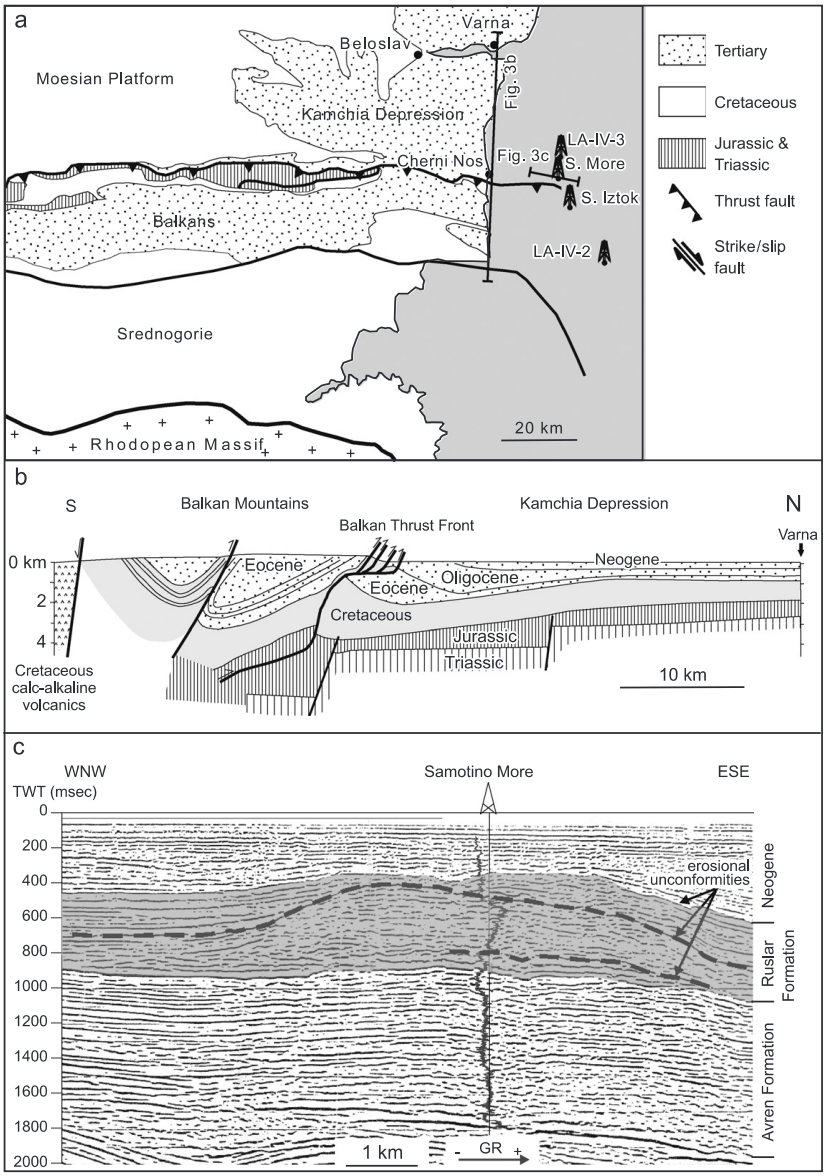

Fig. 3. (a) Map of eastern Bulgaria (Sinclair et al., 1997), showing position of studied offshore wells, (b) S–N trending section through the Balkan Orogene and the Kamchia Depression along the Black Sea coast (simplified after Sinclair et al., 1997) and (c) W–E trending seismic section. The Ruslar Formation is highlighted by grey shading. Note major erosional unconformities within and at the top of the Ruslar Formation. TWT—two-way travel time, GR—gamma ray.

has two cores within this formation (core 1: 462–467 m; core 2: 716–724 m).

In order to study lateral facies variations, samples from Samotino Iztok (drilled in 1984/85), LA-IV-2 (1994) and LA-IV-3 (1995) were included in the study. Collection of cuttings in these wells started only within the Ruslar Formation. Therefore, no samples are available from the upper part of the Ruslar Formation and the overlying Galata Formation. Two cores were taken in the Samotino Iztok well (core 1: 555–562 m; core 2: 562–569 m).

Considerable parts of the Samotino More and Iztok cores are missing. However, a good fit between core data ($calcite_{equiv}$) and log data (conductivity) for Samotino More core 2 (log to core shift: 1.6 m; Fig. 4c) suggests that the depth assignment of at least this core is reliable.

Cuttings from Samotino More and Iztok have been washed and dried at the well site. In contrast, cuttings from LA-IV-2 and LA-IV-3 were wet and contained a lot of gypsum. Therefore, cuttings from the latter two wells had to be washed and gypsum was removed by hand picking.

Calcareous nannoplankton from Samotino More well (14 core samples, 107 cutting samples) was studied in the depth interval from 280 to 1000 m. Semi-quantitative investigations were performed on smear slides, which were prepared using standard techniques. Before preparation small amounts of sediment were treated by ultrasound in distilled water for a few seconds. Smear slides were analysed with a light microscope under 1000 × (Leica DMLP microscope) magnification (cross and parallel nicols).

Powdered samples were analysed for total sulphur (S), total carbon (C), and total organic carbon (TOC, after acidification of samples to remove carbonate) using a Leco CS-300 analyser. The difference between C and TOC is the total inorganic carbon (TIC). TIC contents were used to calculate calcite equivalent ($calcite_{equiv}$) percentages ($= TIC \times 8.34$).

Biogenic silica contents in some samples from the Samotino More well were quantified following a method described by Zolitschka (1998) and were used to calculate opal percentages ($=$ biogenic silica $\times$ 2.4).

Pyrolysis measurements were performed using a "Rock-Eval 2+" instrument. The $S1$ and $S2$ peaks (mgHC/g rock) were used to calculate the hydrogen index ($HI = S2 \times 100/TOC$ [mgHC/gTOC]) and the production index ($PI = S1/(S1 + S2)$; Espitalié et al., 1977). T_{max} was measured as a maturation indicator. For maceral analysis polished blocks of selected core samples were prepared and studied using a Leica microscope.

Twenty-eight core and 10 cuttings samples from the Ruslar Formation were selected for organic geochemical analyses. Representative portions of these samples were extracted for 1 h using dichloromethane in a Dionex ASE 200 accelerated solvent extractor at 75 °C and 50 bar. Asphaltenes were precipitated from a hexane-dichloromethane solution (80:1 according to volume) and separated by centrifugation. The fractions of the hexane-soluble organic matter were separated into saturated and aromatic hydrocarbons and resins using medium-pressure liquid chromatography with a Köhnen–Willsch MPLC instrument (Radke et al., 1980).

The hydrocarbon fractions were analysed by a gas chromatograph equipped with a 30 m DB-5MS fused silica capillary column (i.d. 0.25 mm; 0.25 mm film thickness) coupled to a Finnigan MAT GCQ ion trap mass spectrometer. The oven temperature was programmed from 70 to 300 °C at a rate of 4 °C min^{-1} followed by an isothermal period of 15 min. Helium was used as carrier gas. The mass spectrometer was operated in the electron ionization (EI) mode over a mass range from m/z 50 to m/z 650 (0.7 s total scan time). Identification of individual compounds was accomplished on the basis of retention times in the total ion current chromatogram and comparison of mass spectra with published data. Absolute concentrations of different compound groups were calculated using peak areas from the gas chromatograms in relation to those of internal standards (*deuteriated n-tetracosane* and *1,1′-binaphthyl*, respectively). The concentrations were normalized to TOC.

Carbon isotope measurements of TOC were made after removal of carbonate by concentrated hydrochloric acid. Five to ten mg of each sample were packed in tin capsules and combusted in excess oxygen at 1000 °C using a Roboprep elemental analysers. Residual oxygen was removed by reaction with reduced copper at 600 °C. After passing through a H_2O trap ($MgClO_4$), the resulting CO_2 was analysed online with an European Scientific isotope ratio mass spectrometer. The stable carbon isotope data are presented in the standard denotation relative to PDB with an analytical precision of ± 0.2‰.

Decomposition of calcites for stable carbon and oxygen isotope analyses was carried out by treatment of the pulverized samples with 100% H_3PO_4 in evacuated glass tubes (McCrea, 1950). The reaction time was 12 h and the reaction temperature was kept constant at 25 °C. The stable carbon and oxygen isotope data are presented in the standard denotation relative to PDB with an analytical precision of ± 0.1‰.

4. Results

Geophysical logs of the Ruslar Formation are shown together with the vertical variations of $calcite_{equiv}$ percentages, TOC, and HI values for boreholes LA-IV-3, Samotino More, Samotino Iztok and LA-IV-2 in Figs. 4 and 5. Whereas gamma ray (GR) logs are available for all wells, sonic logs are avialable only for LA wells. Therefore, Induction Logs are shown for the Samotino wells. Analytical results of cores Samotino Iztok 1+2 and Samotino More 2 are presented in Fig. 6.

The Ruslar Formation in the Samotino wells is about 500 m thick and significantly reduced in LA-IV wells. Most probably this is due to Oligocene and post-Oligocene erosion (e.g. Fig. 3c).

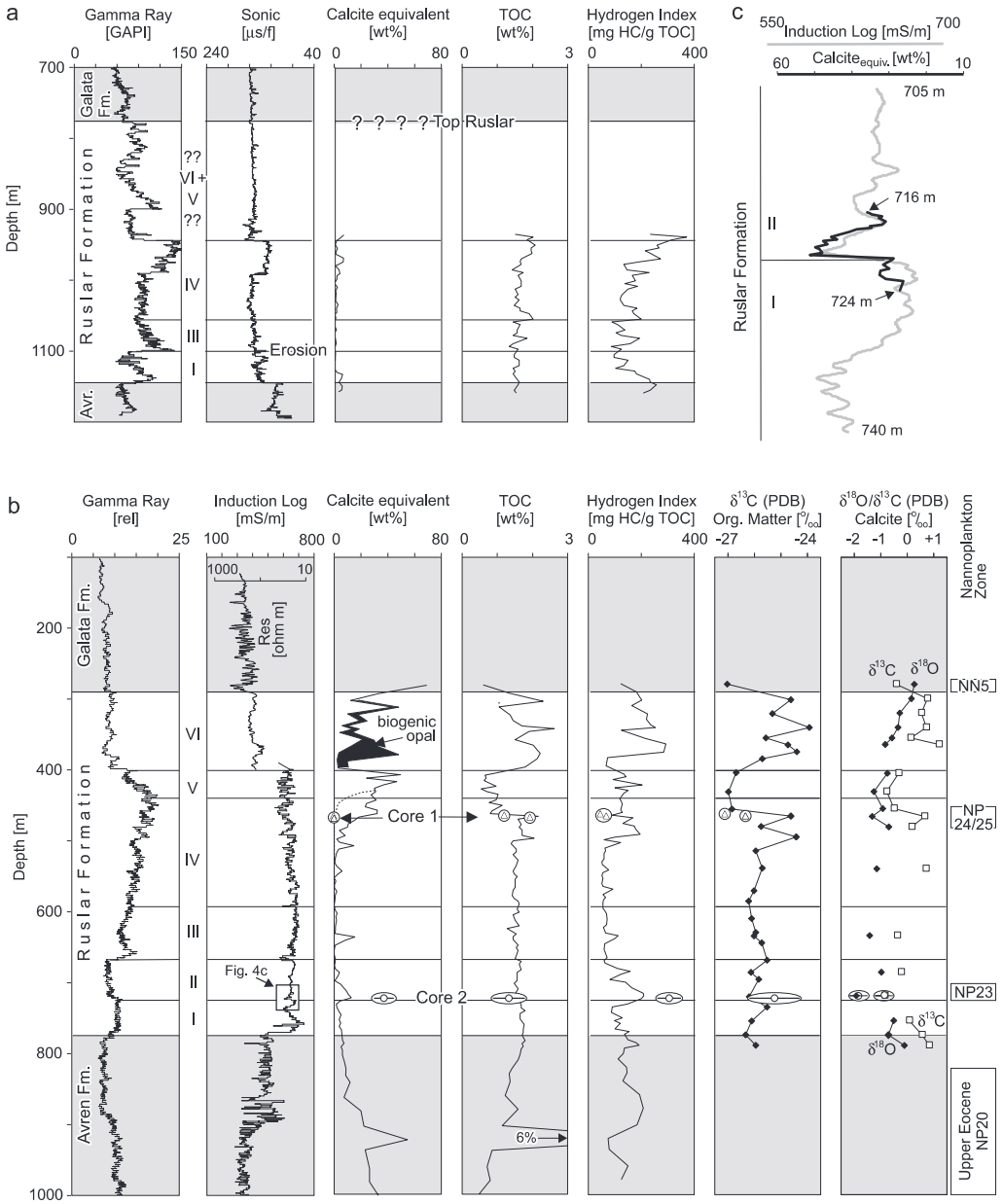

Fig. 4. Well logs and some basic analytical data of (a) LA-IV-3 and (b) Samotino More wells. Isotope data and nannoplankton zones are shown for well Samotino More. Data from Samotino More core 1 (triangles) are shown together with mean values (circles) and standard deviation (bars) of values measured on Samotino More core 2. TOC—total organic carbon. (c) Correlation between Induction Log and carbonate content in Samotino More core 2 (log to core shift: 1.6 m). The good fit shows that the depth assignment is reliable despite of poor core handling.

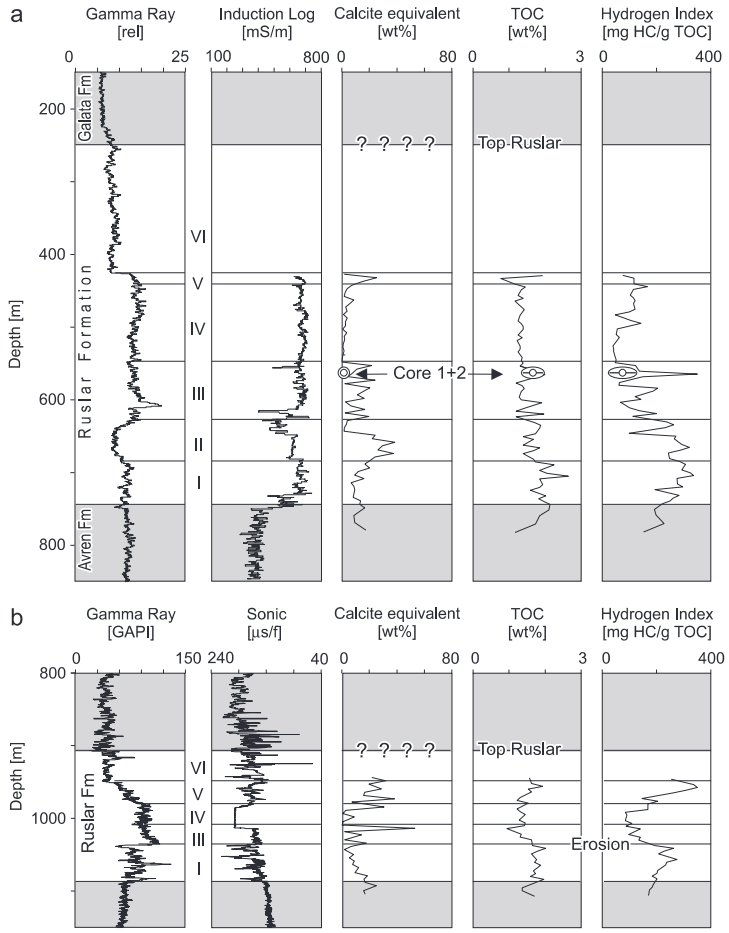

Fig. 5. Well logs and some basic analytical data of (a) Samotino Iztok and (b) LA-IV-2. Mean values (circles) and standard deviation (bars) of values measured on Samotino Iztok core 1 + 2 are shown. TOC—total organic carbon.

4.1. Lithology

Based on geophysical logs and analytical results from the Samotino wells, the Ruslar Formation is subdivided into six units (Figs. 4 and 5). Although less clear, this subdivision is also applied to the LA wells.

- Unit I overlies unconformably the Avren Formation. The 45–60 m thick succession is characterized by moderately high GR values and high electric conductivity. According to cuttings data, unit I is composed of shale with a low carbonate content.
- Unit II is present only in Samotino wells. Sharp breaks in geophysical logs from the LA wells suggest that in these wells unit II is missing due to erosion. In the Samotino wells unit II is about 60 m thick and is characterized by relatively low GR values. Samotino More core 2 represents the lowermost part of unit II. It is composed of bright, dense, marly rocks, which include abundant coccoliths. Cuttings from unit II in the Samotino More well (665–725 m) show a rapid upward decrease in carbonate content. However, because cuttings include less carbonate than core material from the same depth (720 m; Fig. 4b), caving cannot be excluded. With the exception of the uppermost part of unit II (645–635 m), calcareous shale and marls predominate in Samotino Iztok cuttings (Fig. 5a). This suggests a SE-ward increase in carbonate production during deposition of unit II.

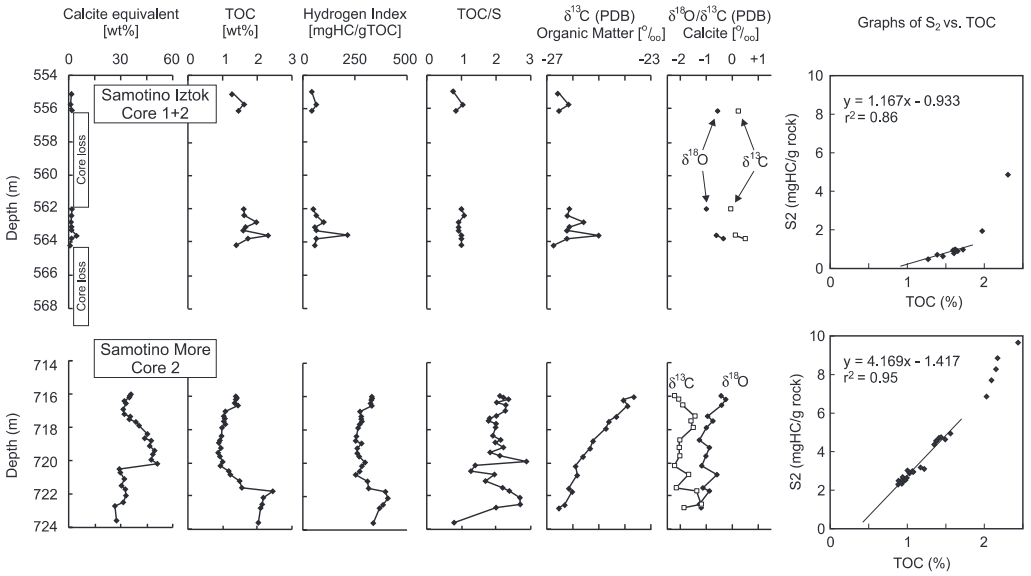

Fig. 6. Calcite equivalent percentages, total organic carbon (TOC) contents, hydrogen index (HI), carbon–sulphur ratios (TOC/S) and isotope data of cores Samotino Iztok 1 + 2 and Samotino More 2. S2 is plotted versus TOC to determine the "true" hydrogen index values of samples with TOC contents below 2%.

- Unit III is characterized by moderately high GR values and attains a thickness of 75–80 m in the Samotino wells (Figs. 4b and 5a). A "warm" shale with high GR readings occurs near the base of unit III, which is mainly composed of laminated shale (e.g. Samotino Iztok cores 1 + 2) with some marly or limy layers. No marls/limestone are found in the north-western LA-IV-3 and Samotino More wells suggesting lateral facies variations.
- Unit IV ranges in thickness from 32 m (LA-IV-2; Fig. 5b) to 162 m (Samotino More; Fig. 4b). It is characterized by high GR values and largely carbonate-free rocks (e.g. Samotino More core 1). Elevated calcite contents in cuttings from the upper part of unit IV in the Samotino More well are probably due to caving from the overlying carbonate rich unit V. The supposed carbonate content between 430 and 490 m depth is indicated by a dotted line in Fig. 4b.
- Unit V is relatively thin (20–30 m). It is characterized by upward decreasing GR values and consists of calcareous shale and marls. Probably, only the lower part of unit V is present in Samotino Iztok.
- Unit VI is the uppermost unit of the Ruslar Formation and is characterized by low GR values. The top of the Ruslar Formation (Oligocene–Miocene boundary) in the Samotino More well at 290 m depth is visible in the Resistivity Log, but hardly recognizable in the Gamma Ray Log (Fig. 4b). In this well, unit VI is ca. 110 m thick and comprises diatomaceous shale with siliceous sponge spicules. Diatoms are especially abundant in the lower part of unit VI (375–365 m), where opal contents reach 45% (Fig. 4b). Because it is difficult to define the upper boundary of unit VI using the Gamma Log alone, the top of the Ruslar Formation is largely speculative in other wells.

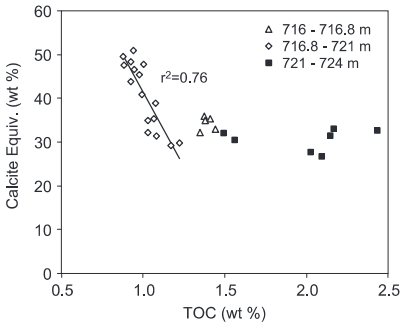

Fig. 7. Calcite content vs. TOC in Samotino More core 2.

The lower part of the Miocene Galata Formation in the Samotino wells is dominated by marl and limestone. It is represented by two cuttings samples from Samotino More.

4.2. Calcareous nannoplankton

Investigations of calcareous nannoplankton have been restricted to the upper part of the Avren Formation,

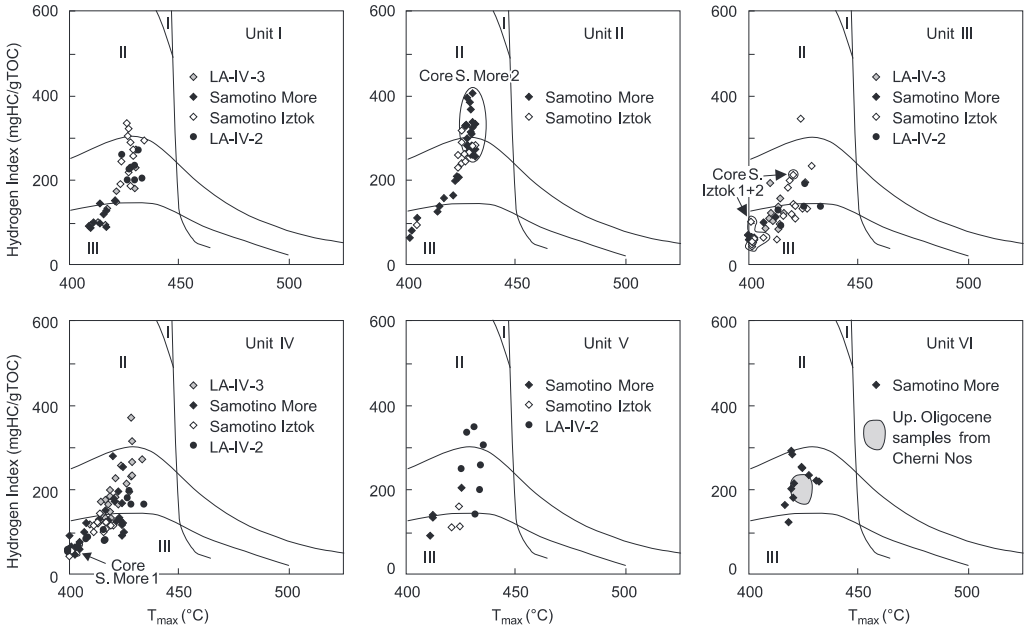

Fig. 8. Hydrogen index (HI) versus T_{max} for units I–VI. Data from outcrop samples collected at Cherni Nos are plotted for comparison together with diatomaceous shales from unit VI.

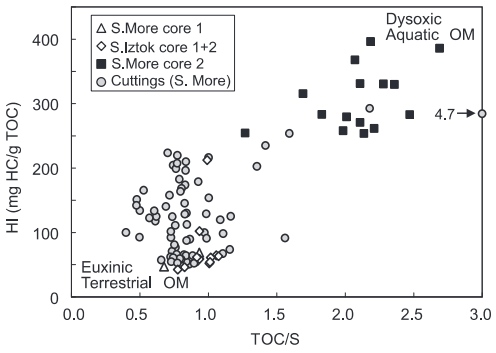

Fig. 9. Hydrogen index (HI) versus the ratio of total organic carbon to total sulphur (TOC/S). Note that samples with high HI values in units II (S. More core 2) and VI are related to high TOC/S ratios. OM—organic matter.

the Ruslar Formation and the Galata Formation in the Samotino More well (Fig. 4b).

4.2.1. Avren Formation

The depth interval from 1000 to 920 m is characterized by common, well preserved nannoplankton: *Coccolithus pelagicus* (Wallich, 1871) Schiller, 1930, *Cyclicargolithus floridanus* (Roth & Hay, 1967) Bukry, 1971, *Ericsonia formosa* (Kamptner, 1963) Haq, 1971, *E. subdisticha* (Roth & Hay, 1967) Roth, 1969, *Isthmolithus recurvus* Deflandre, 1954, *Lanternithus minutus* Stradner, 1962, *Pontosphaera obliquipons* (Deflandre, 1954) Romain, 1979, small reticulofenestrids, *Reticulofenestra bisecta* (Hay, 1966) Roth, 1970, *R. dictyoda* (Deflandre, 1954) Stradner, 1968, *R. hillae* Bukry & Percival, 1971, *R. umbilica* (Levin, 1965) Martini & Ritzkowski, 1968, *Sphenolithus moriformis* (Brönnimann & Stradner, 1960) Bramlette & Wilcoxon, 1967, *Zygrhablithus bijugatus* (Deflandre, 1954) Deflandre, 1959, etc. Rare discoveries of *Discoaster barbardiensis* Tan, 1927 and *D. saipanensis* Bramlette & Riedel, 1954 indicate a Late Eocene age (nannoplankton zone NP20; Perch-Nielsen, 1984). *D. barbardiensis* and *D. saipanensis* also occur in the depth interval from 820 to 900 m, where samples with calcareous nannoplankton are alternating with barren samples. No calcareous nannoplankton has been detected in the uppermost part of the Avren Formation (810–770 m).

4.2.2. Ruslar Formation

Calcareous nannoplankton has been detected in the lower part of unit II (723–700 m) and in the upper part of unit IV (480–450 m). Very rare Miocene nannoplankton in

unit VI (310 m depth) is considered a contamination from the overlying Galata Formation.

Lower part of unit II: Cuttings samples between 720 and 700 m depth and all samples from Samotino More core 2 (723–716 m) are characterized by blooms of endemic nannoplankton with common *Reticulofenestra ornata* Müller, 1970, and regular *Reticulofenestra lockeri* Müller, 1970, *Reticulofenestra* cf. *tokodoensis* Baldi-Beke, 1982, *Pontosphaera multipora* (Kamptner, 1948) Roth, 1970, *P. pax* (Stradner & Seifert, 1980) Aubry, 1986, and *P. fibula* (Gheta, 1976) Aubry, 1986. Rare specimen of small reticulofenestrids, *Braarudosphaera bigelowii* (Gran & Braarud, 1935) Deflandre, 1947, *Reticulofenestra daviesii* (Haq, 1968) Haq, 1971, and *R. umbilica* are restricted to a few samples. Blooms of endemic calcareous nannoplankton with *Reticulofenestra ornata*, *Pontosphaera pax,* and *P. fibula* characterize the lowermost part of NP23 (Lower Solenovian). Mono- and duospecific assemblages of endemic nannoplankton were observed on many localities in the Central and Eastern Paratethys (e.g. Müller, 1970; Krhovský, 1981; Nagymarosy and Voronina, 1991) and have been related to high productivity caused by high nutrient input and decreased salinity.

Upper part of unit IV: Rare nannofossils occur between 480 and 450 m. Based on the occurrence of *Reticulofenestra lockerii* and *Pontosphaera desueta* (Müller, 1970) Perch-Nielsen, 1984, this interval is attributed to the NP24/25 (Upper Solenovian/Kalmykian).

4.2.3. Galata Formation

Samples at 280 and 290 m depth contain a well-preserved nannoflora with *Braarudosphaera bigelowii, Coccolithus pelagicus, Cyclicargolithus floridanus*, reticulofenestrids (*Reticulofenestra minuta* Roth, 1970, *R. pseudoumbilica* (Gartner, 1967) Gartner, 1969), thoracospherids (*Thoracosphaera saxea* Stradner, 1961, *Thoracosphaera heimii* (Lohmann, 1919), Kamptner, 1941), and *Sphenolithus heteromorphus* Deflandre, 1953. The latter has a short stratigraphic range in the Middle Miocene (NN4-NN5). Based on the absence of *Helicosphaera ampliaperta* Bramlette & Wilcoxon, 1967, the lower part of the Galata Formation is attributed to the nannoplankton zone NN5 (Upper Langhian). Reworked Palaeogene and Upper Cretaceous nannoplankton occurs at 290 m depth.

4.3. Bulk geochemical parameters and source potential

TOC contents in the Ruslar Formation vary from 0.5% to 2.7%, but are mostly in the range of 1–2% (Figs. 4–6). Marly layers in units V and VI contain relatively low TOC contents. However, in general there is no good relation between TOC and calcite$_{equiv}$ percentages. A major exception is the middle, marly part of Samotino More core 2 (716.8–721.0 m), where a strong negative correlation exists ($r^2 = 0.76$; Fig. 7). According to Ricken (1991) the negative correlation indicates roughly constant production of organic matter and dilution by varying amounts of calcite. Calcite in this core is mainly derived from calcareous nannoplankton, suggesting a negative correlation between TOC contents and algal blooms.

HI values range from 50 to 400 mgHC/gTOC (Figs. 4–6). Because of the relatively low TOC contents, a mineral-matrix-effect cannot be excluded. In order to test this assumption, *S*2 of core samples is plotted versus TOC in Fig. 6 (Langford and Blanc-Valleron, 1990). The equation of the correlation line suggests that the "true" HI is 417 (S. More core 2) and 117 mgHC/gTOC (S. Iztok core 1 + 2), respectively. These values are higher than the average HI values for these cores (S. More core 2: 304 mgHC/gTOC; S. Iztok core 1 + 2: 74 mgHC/gTOC). A similar mineral–matrix-effect has to be taken into account also in cuttings samples. The differences in HI values between the cores are reflected by different maceral compositions. Lamalginite predominates in Samotino More core 2 and vitrinite predominates in samples from Samotino Iztok core 1 + 2 (and in S. More core 1).

Hydrogen index is plotted versus T_{max} for different units in Fig. 8. The plot shows that the kerogen type varies between II and III and that all samples are immature. Low maturity is also indicated by vitrinite reflectance data varying between 0.25% and 0.35% Rr (Georgiev, G.V., 2004b). The highest HI values occur in Samotino More

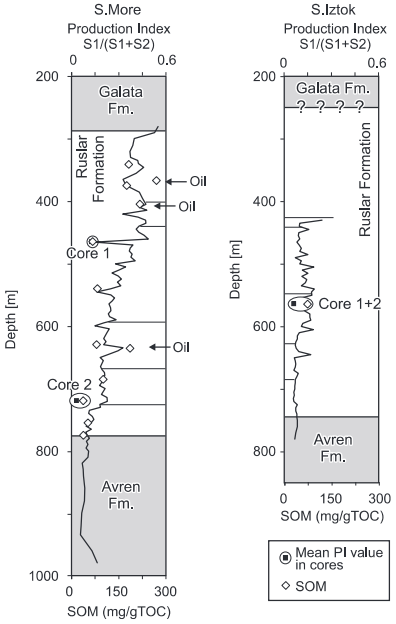

Fig. 10. Production index (PI; solid line) and soluble organic matter (SOM) content normalized to total organic carbon of boreholes Samotino More and Samotino Iztok.

Table 1
Bulk organic geochemical parameters and concentration ratios of selected compounds and compound groups in samples from the Ruslar Formation (bold values indicate-samples from the Avren Formation)

Depth (m)	SOM (mg/gTOC)	Sat HC (wt%, SOM)	Aro HC (wt%, SOM)	NSO (wt%, SOM)	Asph (wt%, SOM)	n-C_{15-19}/n-C_{15-33}	n-C_{21-25}/n-C_{15-33}	n-C_{27-31}/n-C_{15-33}	CPI	Pristane/phytane	Steroids/hopanoids	Aro/sat steroids	Aro/sat hopanoids	di-MTTC/tri-MTTC
Samotino More cuttings														
340	182.4	6	2	82	10	0.54	0.13	0.23	3.2	1.1	0.61	0.20	0.07	n.d.
365	270.2	14	7	67	12	0.14	0.38	0.25	1.1	0.6	1.69	n.d.	n.d.	n.d.
375	174.9	7	2	76	15	0.51	0.12	0.19	1.8	1.1	0.61	0.02	0.02	n.d.
405	218.1	19	5	72	4	0.18	0.31	0.29	1.2	0.8	2.23	n.d.	n.d.	n.d.
540	82.8	10	3	71	16	0.34	0.13	0.29	2.9	1.1	0.73	0.02	0.01	0.26
630	79.8	12	4	66	18	0.41	0.14	0.26	2.8	0.7	0.63	0.15	0.03	0.40
635	185.6	33	12	53	2	0.32	0.30	0.21	1.1	0.6	1.87	n.d.	n.d.	n.d.
685	101.1	7	2	68	23	0.37	0.12	0.26	2.9	1.0	0.82	0.01	0.01	0.32
755	52.9	16	6	64	14	0.36	0.18	0.28	2.1	0.9	0.89	0.05	0.04	0.23
775	38.0	15	5	61	19	0.26	0.15	0.35	2.1	0.9	0.64	0.05	0.03	0.29
1300	**107.0**	**27**	**8**	**57**	**7**	**0.21**	**0.34**	**0.20**	**1.4**	**0.8**	**1.38**	**0.02**	**n.d.**	**n.d.**
1380	**102.6**	**16**	**6**	**73**	**5**	**0.31**	**0.30**	**0.16**	**1.3**	**1.0**	**1.55**	**0.03**	**n.d.**	**0.24**
1420	**426.7**	**5**	**2**	**91**	**2**	**0.29**	**0.35**	**0.13**	**1.3**	**0.9**	**1.41**	**0.03**	**n.d.**	**0.34**
1580	**324.9**	**6**	**2**	**91**	**2**	**0.28**	**0.37**	**0.16**	**1.3**	**1.0**	**1.49**	**0.07**	**0.01**	**0.26**
Samotino More core 1														
463.0	65.9	11	5	73	12	0.27	0.15	0.48	4.7	0.7	0.81	0.02	0.01	0.42
466.0	70.8	7	4	78	12	0.18	0.17	0.50	3.2	0.3	1.10	0.01	0.01	0.33
Samotino More core 2														
716.0	34.2	17	7	50	26	0.19	0.10	0.48	3.6	1.1	0.49	0.12	0.03	0.35
716.2	34.5	19	9	51	21	0.47	0.14	0.33	1.6	1.1	1.03	0.14	0.05	0.12
716.6	40.6	12	7	61	19	0.52	0.11	0.27	1.6	0.9	0.95	0.07	0.04	0.06
717.2	46.6	17	7	63	13	0.48	0.13	0.26	1.8	1.1	0.69	0.08	0.13	0.42
717.5	25.4	18	12	39	31	0.33	0.14	0.29	3.7	1.0	0.87	0.07	0.12	0.25
717.9	35.3	25	9	46	19	0.53	0.15	0.18	3.6	1.0	0.72	0.10	0.23	0.31
718.7	94.7	6	4	40	49	0.32	0.08	0.28	3.0	1.0	0.63	0.12	0.14	0.16
719.1	37.9	15	9	38	38	0.19	0.13	0.34	3.6	1.2	0.92	0.16	0.12	0.21
719.6	46.5	12	6	36	46	0.20	0.11	0.39	2.3	1.1	0.99	0.09	0.14	0.06
720.7	48.9	24	12	47	17	0.51	0.12	0.20	2.2	1.5	1.21	0.08	0.12	0.05
720.7	48.8	27	11	47	15	0.45	0.15	0.18	1.6	1.3	0.81	0.05	0.09	0.17
721.5	19.6	24	10	50	16	0.52	0.12	0.17	1.7	1.3	0.63	0.24	0.25	0.29
721.7	27.2	17	7	64	13	0.55	0.09	0.24	1.6	1.2	0.83	0.13	0.16	0.34
722.5	23.7	14	7	68	11	0.67	0.12	0.09	n.d.	1.4	0.66	0.19	0.21	0.26
722.7	40.2	9	3	68	20	0.52	0.10	0.29	2.8	1.5	0.51	0.22	0.14	0.21
Samotino Iztok core 1														
555.0	101.1	6	3	78	14	0.25	0.15	0.46	4.2	0.6	1.18	0.02	0.02	0.39
555.7	65.2	5	3	69	23	0.16	0.16	0.55	3.2	0.4	1.58	0.02	0.02	0.51
556.1	84.5	3	2	70	25	0.19	0.15	0.55	3.1	0.6	1.56	0.01	0.01	0.49
Samotino Iztok core 2														
562.1	81.6	4	2	67	27	0.17	0.15	0.55	3.7	0.4	1.89	0.02	0.03	0.40
562.5	69.6	8	3	67	23	0.14	0.11	0.48	1.5	0.4	1.36	0.02	0.01	0.43
562.9	70.6	3	2	70	24	0.15	0.31	0.37	3.2	0.4	1.14	0.03	0.01	0.38
563.1	77.5	4	2	71	24	0.15	0.08	0.45	2.8	0.4	1.95	0.01	0.01	0.26
563.3	80.2	4	1	73	22	0.21	0.15	0.51	3.5	0.3	2.49	0.01	0.01	0.32
563.6	30.4	8	6	77	10	0.24	0.08	0.36	3.2	0.4	1.71	0.02	0.01	0.48
563.9	79.8	4	2	66	28	0.15	0.09	0.44	3.3	0.3	2.64	0.02	0.02	0.52
564.2	95.2	3	1	70	26	0.11	0.09	0.45	3.5	0.6	0.96	0.02	0.02	0.38

SOM = soluble organic matter, Sat = saturated, Aro = aromatic, HC = hydrocarbons, NSO = NSO compounds, Asph = asphaltenes, CPI = carbon preference index (according to Bray and Evans, 1961), di-MTTC = dimethylated C_{29}-chroman, tri-MTTC = trimethylated C_{29}-chroman, TOC = total organic carbon, n.d. = not detectable.

core 2 (716–724 m). Overall positive relationships exist between HI and T_{max} values (Fig. 9). These probably are caused by the lower T_{max} values characteristic for immature type III kerogen in comparison to type II kerogen (e.g. Peters, 1986). However, an additional reduction of T_{max} due to organic sulphur incorporation cannot be excluded. The presence of thiophenes in the aromatic hydrocarbons of Samotino Iztok core 1 + 2 and Samotino

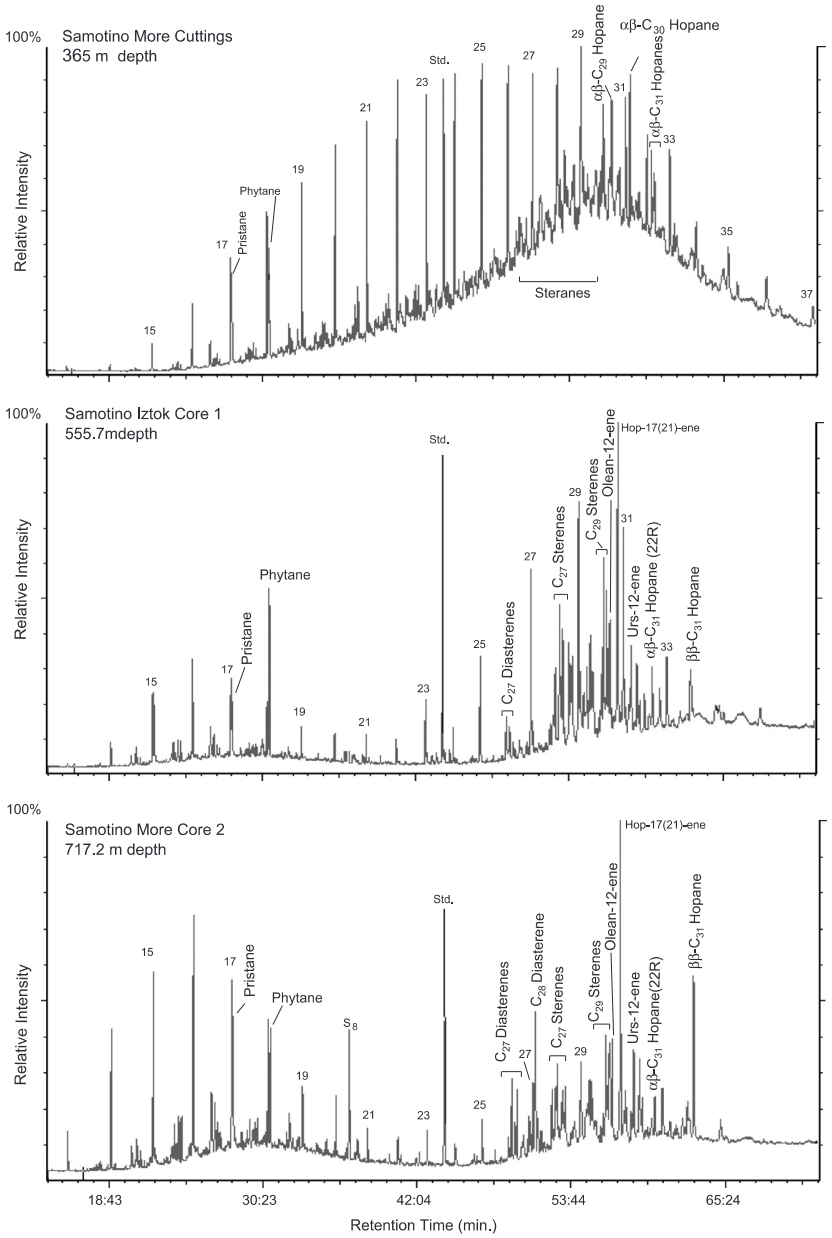

Fig. 11. Gas chromatograms (total ion current) of the saturated hydrocarbon fractions. *n*-Alkanes are labelled according to their carbon number. Std., standard (deuterated *n*-tetracosane).

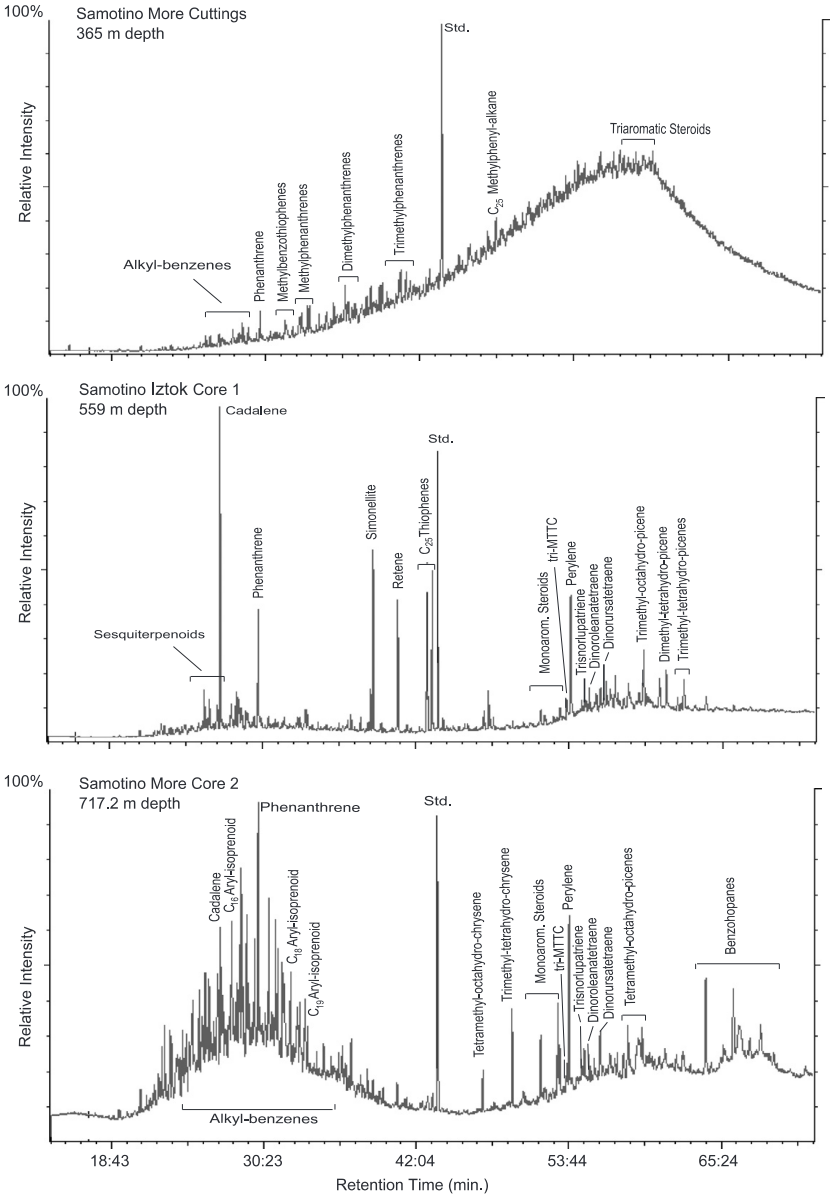

Fig. 12. Gas chromatograms (total ion current) of the aromatic hydrocarbon fractions. Std., standard (1,1′-binaphthyl).

More core 1 (see discussion under Section 4.5.2) is an indication for enhanced organic sulphur incorporation.

The ratios of total organic carbon to total sulphur contents (TOC/S) are in the range of 0.7–2.7. Empirical investigations relate TOC/S ratios of about 2.8 to "normal marine" conditions, whereas values 5 2.8 may be indicative for euxinic conditions (Berner, 1984). Interestingly, an overall tendency toward higher HI values with increasing

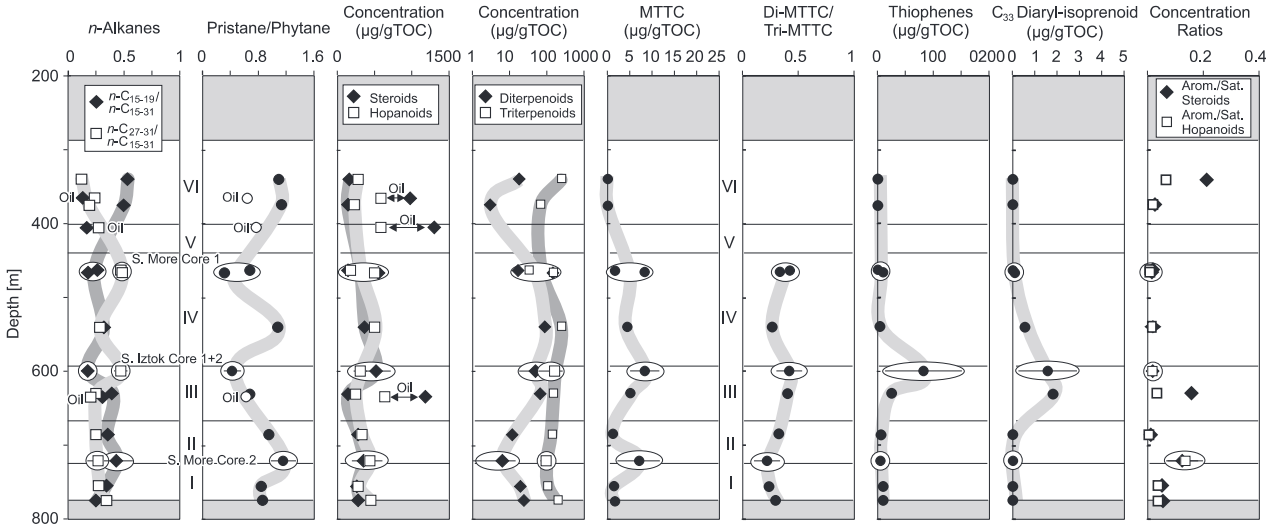

Fig. 13. Biomarker proxies of cuttings and core samples in well Samotino More. Mean values and standard deviation are displayed for cores Samotino More 2 and Samotino Iztok 1 + 2. The latter cores have been projected into the Samotino More well. Cuttings samples contaminated by a mature oil are labelled.

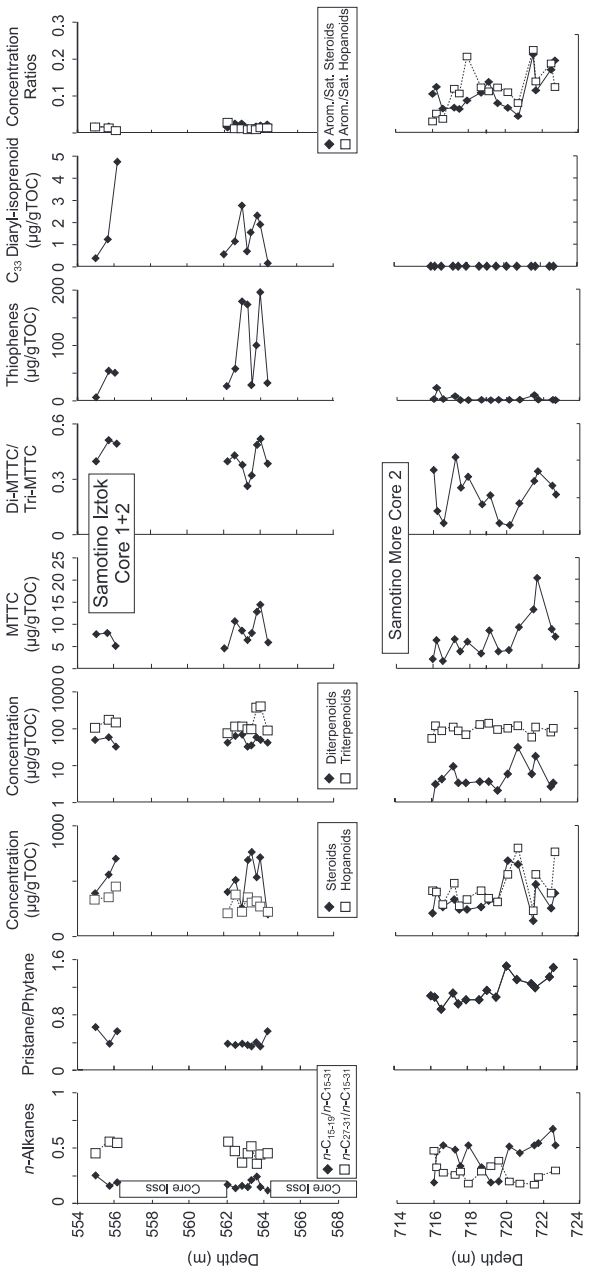

Fig. 14. Biomarker proxies of cores Samotino Iztok 1 + 2 and Samotino More 2.

TOC/S ratios exists within the Ruslar Formation (Fig. 9). The differences are clearly seen by comparing the results of the samples from S. Iztok core 1+2 and S. More core 2 (Fig. 6). Low TOC/S ratios are associated with relatively low TOC and low HI values, contrary to the relationships normally found in anoxic/euxinic environments. Variations in TOC/S ratios may be partly caused by differences in the metabolizability of organic matter by sulphate-reducing bacteria. Refractory terrestrial organic matter could result in high TOC/S ratios. However, in the present case low HI values (high terrestrial OM contents) are found in samples with low TOC/S ratios and TOC/S shows no relationship with TOC. Elevated TOC/S ratios in the S. More core 2 may partly reflect lower pyrite sulphur incorporation due to Fe-limitation in more calcareous facies (e.g. Dean and Arthur, 1989), as indicated by the high carbonate contents of the samples.

The results are interpreted to reflect variations in the position of the chemocline (i.e. within the sediment or within the water column; dysoxic versus euxinic conditions) during deposition of the sediments and in the ratios of allochthonous (e.g. land plants) versus autochthonous organic matter (e.g. algae) input.

4.4. Free hydrocarbons

All samples are immature. Therefore, a low Production Index (PI;○ 0.1) has to be expected. However, significantly higher values are recorded for samples from well Samotino More, where a conspicuous upward increase in PI is observed in the Ruslar Formation (Fig. 10). Relatively high PI values also occur in the shallow Samotino More core 1. However, PI values in Ruslar cores are generally lower than in Ruslar cuttings (Fig. 10). Despite of a subtle increase in PI between 650 and 550 m depth, a general upward increase in PI values within the Ruslar Formation cannot be observed in the Samotino Iztok well (Fig. 10). PI values of LA wells are constantly below 0.1 without any anomalous data.

Rock extracts from core and cuttings samples from the Ruslar Formation in the Samotino More well have been investigated to study the origin of the free hydrocarbons. All core and most cuttings samples yielded chromatograms characteristic for samples with a low maturity. However, cuttings samples at 365, 405 and 635 m depth show a strong contamination by a mature oil, indicated by high TOC-normalized yields of soluble organic matter (SOM; Fig. 10) and high relative proportions of saturated hydrocarbons (Table 1).

The GC traces of the saturated hydrocarbon fractions of the contaminated samples are dominated by *n*-alkanes in the *n*-C_{22}–*n*-C_{29} range, 17a, 21a(H)-type hopanes and regular C_{27}–C_{29}-steranes (Fig. 11). In contrast to the rest of the sample set from the Ruslar Formation, the long-chain *n*-alkanes are characterized by a slight odd-over even-predominance (CPI = Carbon Preference Index (according to Bray and Evans, 1961) between 1.1 and 1.2; Table 1). The relative proportions of *S*/*R* isomers of the C_{29} steranes and the C_{31} hopanes are consistent with a thermal maturity equivalent to vitrinite reflectance values of approximately 0.8% Rr (Mackenzie and Maxwell, 1981). The aromatic hydrocarbon fractions of the oil-impregnated samples are characterized by high proportions of an irresolvable complex mixture (hump) with only few individual compounds of higher relative intensities (Fig. 12). Using the MPI 1 (Radke and Welte, 1983), an equivalent vitrinite reflectance of 0.82–0.85% Rr (Radke et al., 1984) has been determined for these oils, which is further supported by the predominance of triaromatic over monoaromatic steroids (Fig. 12).

Another PI anomaly occurs in the Samotino More well within the Avren Formation between 1420 and 1680 m depth. Whereas the PI is about 0.1 above the anomaly, it is 0.4–0.5 within the anomaly. Extracts from two samples above and within the anomaly have been investigated in order to compare them with extracts from the anomaly within the Ruslar Formation. As expected the SOM yield is very high in the samples from the anomaly (Table 1). In contrast to Ruslar samples, the extract in the anomalous zone in the Avren Formation is dominated by NSO-compounds, whereas the absolute content in saturated and aromatic hydrocarbons is similar to that detected in Avren samples above the anomaly (Table 1). Free hydrocarbons in the anomalous zones in the Ruslar and Avren formations, therefore, have a different source.

The origin of the oil in the Avren and Ruslar formations remains unclear. Gas and condensate have been tested from Eocene rocks (e.g. at 1720–1785 m depth). Therefore, we speculate that the NSO-rich oil is a migration residue. According to drilling reports, no oil had been added to the drilling mud. Therefore, oil stains in the Ruslar Formation may be derived from an undetected shallow oil accumulation. However, a contamination cannot be excluded.

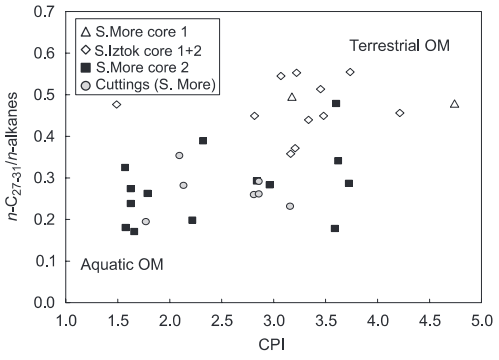

Fig. 15. Cross-plot of the proportion of long-chain *n*-alkanes versus Carbon Preference Index (CPI; according to Bray and Evans, 1961).

4.5. Organic geochemistry

Drill core samples from all core intervals recovering sediments of the Ruslar Formation were investigated for their molecular composition of hydrocarbons (Fig. 14). In order to obtain comparable information from additional lithological units, 10 cutting samples were selected for organic geochemical analyses (Table 1; Fig. 13). Three samples were identified as oil impregnated (see Section 4.4) and are therefore excluded from the discussion with regard to sedimentary facies reconstruction. The hydrocarbon compositions of the two remaining cutting samples from unit VI (340 and 375 m depth) are slightly influenced by oil. However, their biomarker signatures (except of possibly the *n*-alkane patterns and the pristane/phytane ratios) can be used for facies reconstruction.

Table 2
Concentration of biomarkers of cutting and core samples from the Ruslar Formation (bold values indicate samples from the Avren Formation)

Depth (m)	*n*-Alkanes (mg/g TOC)	Sterenes (mg/g TOC)	Diasterenes (mg/g TOC)	Hopanes (mg/g TOC)	Hop-17(21)-ene (mg/g TOC)	Monoarom. steroids (mg/g TOC)	Benzohopanes (mg/g TOC)	Thiophenes (mg/g TOC)	MTTC (mg/g TOC)	C_{33}-Diaryl-isoprenoid (mg/g TOC)	Diterpenoids (mg/g TOC)	Triterpenoids (mg/g TOC)
Samotino More cuttings												
340	852	100	40	204	52	27.6	17.0	n.d.	n.d.	n.d.	17.3	259.1
365	3778	638	328	526	45	n.d.	n.d.	n.d.	n.d.	n.d.	n.d.	n.d.
375	811	91	43	169	52	3.3	4.0	n.d.	n.d.	n.d.	2.8	70.8
405	1880	891	410	568	14	n.d.	n.d.	n.d.	n.d.	n.d.	n.d.	n.d.
540	824	259	90	372	109	6.7	6.9	3.2	4.3	0.56	85.0	254.0
630	646	79	51	160	69	19.6	7.7	24.6	5.1	1.78	64.0	149.2
635	2669	791	382	564	65	n.d.	n.d.	n.d.	n.d.	n.d.	n.d.	n.d.
685	585	184	76	236	84	2.9	1.7	4.8	1.2	n.d.	11.4	139.2
755	669	156	80	206	65	12.4	9.7	8.9	1.3	n.d.	18.7	110.3
775	565	180	83	327	94	13.6	14.6	9.2	1.6	n.d.	24.4	199.5
1300	**972**	**600**	**238**	**547**	**74**	**18.2**	**n.d.**	**n.d.**	**n.d.**	**n.d.**	**32.0**	**224.6**
1380	**485**	**335**	**79**	**254**	**21**	**10.6**	**n.d.**	**n.d.**	**2.8**	**n.d.**	**9.6**	**169.4**
1420	**794**	**523**	**124**	**435**	**36**	**16.6**	**n.d.**	**n.d.**	**3.1**	**n.d.**	**16.7**	**218.3**
1580	**611**	**362**	**76**	**296**	**14**	**30.9**	**4.4**	**n.d.**	**7.0**	**n.d.**	**18.3**	**85.7**
Samotino More core 1												
463.0	299	101	36	131	40	2.5	1.4	0.3	1.5	n.d.	16.9	35.1
466.0	504	338	197	349	139	7.9	4.1	9.0	8.2	0.11	140.6	150.3
Samotino More core 2												
716.0	349	178	6	309	84	21.9	13.2	0.9	2.2	n.d.	0.7	51.0
716.2	452	288	71	245	133	49.7	20.7	20.2	6.1	n.d.	3.1	115.4
716.6	349	202	47	171	99	17.8	11.3	1.1	1.7	n.d.	4.3	82.2
717.2	531	220	85	282	134	23.0	55.5	6.6	6.6	n.d.	9.0	111.5
717.5	196	137	76	159	87	16.3	29.1	n.d.	3.9	n.d.	3.4	84.3
717.9	374	153	65	184	84	21.3	62.8	n.d.	6.0	n.d.	3.3	65.4
718.7	595	169	62	281	80	28.2	49.9	n.d.	3.3	n.d.	3.5	131.2
719.1	355	181	96	210	98	43.3	38.3	n.d.	8.4	n.d.	3.6	142.1
719.6	321	194	86	202	68	24.9	37.5	n.d.	3.7	n.d.	2.0	89.6
720.7	1053	518	112	387	113	47.6	61.8	n.d.	4.1	n.d.	5.7	98.8
720.7	1091	432	184	611	121	31.5	65.9	n.d.	9.2	n.d.	30.1	114.7
721.5	253	83	29	128	49	26.7	44.6	8.7	13.2	n.d.	6.0	58.1
721.7	377	322	86	328	150	52.2	74.6	n.d.	20.4	n.d.	17.4	108.1
722.5	170	175	39	229	89	41.1	66.6	n.d.	8.6	n.d.	2.5	80.4
722.7	312	274	46	296	373	70.2	92.6	n.d.	7.2	n.d.	3.3	96.2
Samotino Iztok core 1												
555.0	530	252	132	213	111	6.8	5.8	6.0	7.8	0.37	49.2	99.9
555.7	528	356	191	233	115	10.1	5.3	53.9	8.1	1.21	55.2	166.3
556.1	688	463	227	283	159	4.9	2.6	50.8	5.1	4.72	31.6	148.1
Samotino Iztok core 2												
562.1	381	246	144	122	82	7.2	6.5	26.8	4.5	0.55	42.2	72.7
562.5	681	319	170	264	101	12.1	4.4	57.0	10.6	1.12	63.6	111.1
562.9	399	184	59	106	111	6.4	2.6	179.3	8.5	2.74	67.9	112.1
563.1	501	456	225	255	95	6.9	2.8	174.4	6.3	0.66	32.4	94.5
563.3	481	433	313	206	94	8.9	3.3	27.0	7.9	1.54	34.7	94.8
563.6	342	295	229	209	101	9.2	2.3	100.8	12.7	2.30	58.4	356.4
563.9	351	408	295	188	79	13.4	4.1	196.1	14.3	1.89	50.1	397.5
564.2	352	160	43	147	67	4.9	3.3	31.9	5.8	0.13	39.6	89.5

TOC = total organic carbon, MTTC = di- plus tri-methylated C_{29} chromans, n.d. = not detectable.

4.5.1. Bulk organic geochemical parameters

The normalized yields of the SOM of the studied samples are listed in Table 1 together with the relative proportions of saturated and aromatic hydrocarbons, NSO compounds and asphaltenes of the SOM. The SOM yields of the samples not influenced by oil impregnation vary between 19.6 and 101.1 mg/g TOC (Table 1). The relative proportions of hydrocarbons of the SOM from the Samotino More core 1, the Samotino Iztok core 1 + 2, and the cutting samples from 340 to 685 m are low (4–16%), consistent with the low maturity of the organic matter (Table 1). The soluble organic matter is mainly composed of NSO compounds (4 65% of the SOM) and asphaltenes (10–28%). In the Samotino More core 2 and the Samotino More cutting samples from 755 to 775 m, higher relative proportions of hydrocarbons are obtained (10–38%).

4.5.2. Molecular composition of hydrocarbons

n-Alkanes and isoprenoids—The *n*-alkane patterns of the samples from the S. More core 1 and the S. Iztok core 1 + 2 are dominated by long-chain *n*-alkanes (4 *n*-C_{27}; Fig. 11) with a marked odd over even predominance (CPI: 1.5–4.7) and maximum intensities in the *n*-C_{29}–*n*-C_{31} range (Fig. 11). In contrast, the samples from the Samotino More core 2 (Fig. 11) and from most of the non-oil cuttings are dominated by short-chain (○ *n*-C_{20}) *n*-alkanes or show equal relative abundance of short- and long-chain homologues (Table 1).

High proportions of long-chain C_{27}–C_{31} *n*-alkanes relative to the sum of *n*-alkanes (Figs. 12 and 13) are typical for higher terrestrial plants, where they occur as the main components of plant waxes (Eglinton and Hamilton, 1967). The occurrence of short-chain *n*-alkanes (○ C_{20}) in high amounts (19–67% of the total *n*-alkane concentrations) in the Samotino More core 2 (Fig. 14) argues for a predominant origin of organic matter from algae and microorganisms (Cranwell, 1977). The differences in terrestrial (allochthonous) organic matter input versus aquatic (autochthonous) organic matter production are further reflected by generally lower CPI values of the samples characterized by low relative proportions of long-chain *n*-alkanes (Fig. 15).

According to Didyk et al. (1978), pristane/phytane ratios below 1.0 indicate anaerobic conditions during early diagenesis, and values between 1.0 and 3.0 were interpreted as reflecting dysaerobic environments. However, pristane/phytane ratios are known to be also affected by maturation (Tissot and Welte, 1984) and by differences in the precursors for acyclic isoprenoids (i.e. bacterial origin; Volkman and Maxwell, 1986; ten Haven et al., 1987). A major influence of different ranks on pristane/phytane ratios can be ruled out within the Ruslar Formation. In the present case, the pristane/phytane ratios are interpreted to reflect differences in the redox conditions of the samples, because of independent molecular indicators of water column anoxia in samples characterized by low pristane/phytane ratios (see sections thiopenes and aryl- and diaryl isoprenoids). However, a bacterial origin of phytane from phytanyl ether lipids found in archaebacteria as well as the formation of pristane from tocopherols (vitamin-E) or chromans (Goossens et al., 1984) cannot be excluded. The pristane/phytane ratios show moderate variability between 0.7 and 1.5 within most samples (Table 1). Values below 0.7 are exclusively obtained within samples from the Samotino Iztok core 1 + 2 and one sample from the Samotino More core 1 (Figs. 12 and 13), arguing for anoxic conditions in the bottom water during the deposition of these sediments. Differences in redox conditions during deposition of S. Iztok core 1 + 2 and S. More core 2 samples are most probably related to the presence/absence of free H_2S in the water column, as suggested by differences in the TOC/S ratios of the core samples (Figs. 5 and 13) and the presence of thiophenes in the aromatic hydrocarbon fractions.

Steroids and hopanoids—The sediments of the Ruslar Formation are characterized by the occurrence of C_{27}–C_{29}

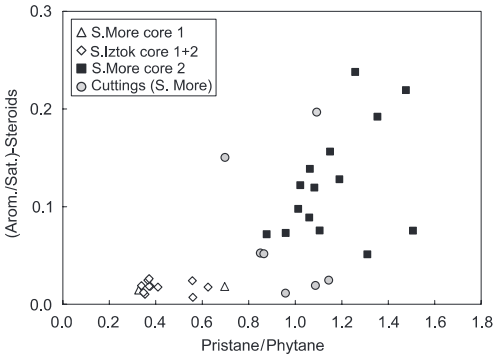

Fig. 16. Aromatic/saturated steroids ratio versus the pristane/phytane ratio.

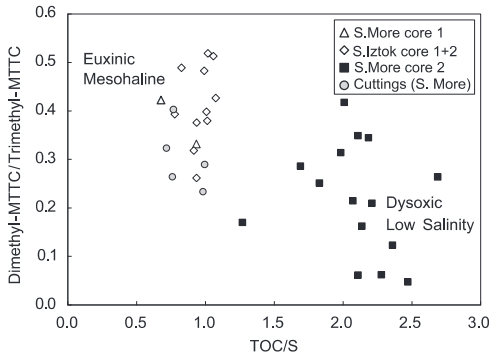

Fig. 17. Dimethyl-MTTC/Trimethyl-MTTC ratio versus the total organic carbon and total sulphur ratio (TOC/S).

(D^4, D^5)-sterenes and the corresponding diaster-13(17)-enes in moderate to high contents in the non-aromatic hydrocarbon fractions (Table 2; Fig. 11). In addition, 5a(H)- and 5b(H)-type regular C_{27}–C_{29}-steranes are present in low quantities. In the aromatic hydrocarbon fractions (Fig. 12), monoaromonatic steroids were identified (Table 2). These compounds arise from the early diagenetic transformation of sterols and subsequent aromatization of ring-C (Mackenzie et al., 1981).

Algae have been discussed as the predominant primary producers of C_{27}-sterols, while C_{29}-sterols are more typically associated with land plants (Volkman, 1986). In the present case, C_{29} and C_{27} steroids are present in nearly equal abundance, consistent with a mixed algal-terrestrial organic matter input. On average, steroids are present in higher concentrations within the Samotino Iztok core 1 + 2 (Fig. 14).

The hopanoid patterns are characterized by the occurrence of 17a, 21b(H)- and 17b, 21b(H)-type hopanes from C_{27} to C_{32} with the C_{28} hopanes being absent (Table 2; Fig. 11). The predominant hopanoids in most of the samples are the hop-17(21)-ene and the 17b, 21b(H)-homohopane (Fig. 11). Two series of benzohopanes cyclized at the C(20) and the C(16) position, respectively (Hussler et al., 1984; Schaeffer et al., 1995), were identified in the aromatic hydrocarbon fractions (Fig. 12) of the samples (Table 2).

The most probable biological precursor of the hopane derivatives found in the samples is bacteriohopanepolyols (Ourisson et al., 1979; Rohmer et al., 1992). These compounds have been identified in bacteria, as well as in some cryptogames (e.g. moss, ferns).

Both core profiles differ in steroids/hopanoids ratios, a measure of organic matter production by autothrophic eukaryotes (e.g. algae, land plants) versus bacterial activity (Fig. 14). Low sterane/hopane ratios are considered to indicate a lacustrine or a special, bacteria-influenced facies, whereas a high ratio is indicative of a marine organic facies (Mackenzie, 1984). An influence of freshwater during deposition of the Samotino More core 2 samples may be indicated by the concentration ratios of 2-methyl-2-trimethyl-tridecylchromans (MTTCs; see section Chromans).

Further differences are seen in the extent of aromatization of steroids and hopanoids, especially by comparing the results of drill core samples (Fig. 14). Because of negligible differences in thermal maturity and a lower potential of the clay catalytic effect on aromatization in the carbonate-rich Samotino More core 2, the higher degree of aromatization of steroids and hopanoids is most probably related to differences in redox conditions. This interpretation is supported by the fact that higher ratios of aromatic versus saturated steroids are obtained from samples characterized by higher pristane/phytane ratios (Fig. 16).

Sesquiterpenoids, diterpenoids and non-hopanoid triterpenoids—In all samples of the Ruslar Formation investigated (except of the oil-impregnated cuttings), aromatic sesquiterpenoids of the cadinane-type dominated by cadalene (Fig. 12), are observed (Simoneit and Mazurek, 1982). The aromatic diterpenoids (Fig. 12) consist of compounds of the abietane type (e.g. simonellite, retene; Philp, 1985) indicating a contribution of OM from conifers.

Non-hopanoid triterpenoids containing the structures typical of the oleanane, ursane, or lupane skeletons (Figs. 11 and 12) were identified in the hydrocarbon fractions (Spyckerelle et al., 1977; LaFlamme and Hites, 1979; Wakeham et al., 1980; Wolff et al., 1989; ten Haven et al., 1992; Logan and Eglinton, 1994; Philp, 1985; Rullkötter et al., 1994). These compounds are known as biomarkers for angiosperms (Karrer et al., 1977; Sukh Dev, 1989).

The absolute concentrations of diterpenoids in the samples of the Ruslar Formation are lower than the contents of angiosperm-derived triterpenoids (Table 2; Figs. 12 and 13). Very low contents of resinous organic matter from conifers in relation to angiosperm-derived material are found in the Samotino More core 2 (Fig. 14). Consistent with the differences in *n*-alkanes distribution patterns (Fig. 11), the absolute concentrations of land-plant-derived terpenoid biomarkers (di- plus angiosperm-derived triterpenoid hydrocarbons) are lower in the S. More core 2 compared with the results of the Samotino Iztok core 1 + 2 samples (Table 2).

Chromans—In a series of methylated 2-methyl-2-(trimethyltridecyl)chromans (MTTC), the 2,5,7,8-tetramethyl-2-(4′,8′,12′-trimethyltridecyl)chroman (tri-MTTC) occurs in most of the samples (except of samples from unit VI) in low amounts (Table 2). It predominates over the 2,5,8-trimethyl-2-(4′,8′,12′-trimethyltridecyl)chroman (di-MTTC) (Sinninghe Damsté et al., 1987; Schwark and Püttmann, 1990).

The depth-trends of MTTC concentrations and the di-MTTC/tri-MTTC ratios (Table 1) within the Ruslar Formation indicate units characterized by slightly enhanced salinity (Fig. 13). Euhaline to mesohaline (~35–40‰) conditions are suggested during deposition of sediments of the Samotino More core 1 and the Samotino Iztok core 1 + 2 (Figs. 12 and 13), whereas the results of the S. More core 2 samples argue for on average lower salinity. The results are consistent with brackish conditions in the surface water but a still existing salinity stratification in the water column (Sinninghe Damsté et al., 1993). The differences are best illustrated by a cross-plot of the dimethylated-MTTC to trimethylated-MTTC concentrations versus the TOC/S ratios (Fig. 17). The diagram outlines the correspondence of euxinic conditions in the bottom water with enhanced salinity within the depositional environment.

Thiophenes—Two C_{25} highly branched isoprenoid thiophenes (Sinninghe Damsté et al., 1989) occur within the samples from the S. Iztok core 1 + 2 in highly variable concentration (6–200 mg/g TOC; Fig. 14), and in generally lower contents (0.3–20 mg/g TOC) within the samples from the S. More core 1 and the uppermost samples from the S. More core 2, as well as in the cutting samples below 540 m (Table 3).

Table 3
Carbon isotopic composition of total organic carbon (TOC), as well as carbon and oxygen isotopic composition of carbonate (Carb) of cutting and core samples from the Ruslar Formation

Depth (m)	$d^{13}C_{TOC}$ (‰, PDB)	$d^{13}C_{Carb}$ (‰, PDB)	$d^{18}O_{Carb}$ (‰, PDB)
Samotino More cuttings			
280	−27.0	−0.4	0.3
300	−24.6	0.8	0.2
320	−25.3	0.5	−0.3
340	−23.9	0.7	−0.3
355	−25.6	0.1	−0.6
365	−24.7	1.2	−0.8
375	−24.4		
385	−25.7		
405	−26.7	−0.3	−0.8
430	−27.0	−0.8	−1.3
455	−26.8	−0.5	−0.9
465	−25.4	0.7	−1.3
480	−25.7	0.2	−0.7
495	−25.4		
515	−25.9		
540	−25.7	0.7	−1.2
570	−26.0		
585	−26.2		
610	−26.1		
630	−25.9		
635	−26.0	−0.4	−1.4
645	−25.7		
670	−25.5		
685	−26.1	−0.2	−1.0
695	−25.8		
720	−26.2	−0.8	−1.9
735	−25.5		
755	−26.1	0.1	−0.5
775	−26.3	0.6	−0.7
790	−25.9	0.8	−0.1
Samotino More core 1			
463.0	−27.1		
466.0	−26.3		
Samotino More core 2			
716.0	−23.7	−0.4	−2.2
716.2	−24.1	−0.3	−2.1
716.6	−23.9	−0.4	−1.9
717.2	−24.3	−0.9	−1.5
717.5	−24.6	−0.8	−1.6
717.9	−24.7	−1.0	−1.5
718.7	−25.2	−1.3	−2.0
719.1	−25.3	−0.9	−2.0
719.6	−25.6	−1.0	−2.0
720.7	−25.9	−1.2	−2.2
720.7	−25.8	−0.6	−1.7
721.5	−26.2	−1.1	−2.2
721.7	−26.0	−0.9	−1.4
722.5	−26.3	−1.3	−1.2
722.7	−26.5	−1.2	−1.9
Samotino Iztok core 1			
555.0	−26.6		
555.7	−26.2		
556.1	−26.5	0.2	−0.6
Samotino Iztok core 2			
562.1	−26.1	−0.1	−1.0
562.5	−26.2		
562.9	−25.6		
563.1	−26.1		
563.3	−26.2		
563.6	−25.0	0.1	−0.6
563.9	−26.2	0.5	−0.3
564.2	−26.7		

Within the Ruslar Formation high concentrations of thiophenes are measured in samples yielding enhanced di-MTTC/tri-MTTC ratios (Fig. 13). The thiophenes identified are suggested to have been formed by selective sulphur incorporation reactions into highly branched isoprenoid alkenes, favoured by the presence of free H_2S in the water column (Sinninghe Damsté et al., 1989). The results support the conclusion about the establishment of euxinic conditions due to intensified salinity stratification in the water column, as further indicated by low pristane/phytane ratios of the samples with high thiophenes contents (Fig. 18a).

Aryl- and diaryl isoprenoids—The aromatic hydrocarbon composition is further characterized by the occurrence of trimethyl-substituted aryl isoprenoids in the range C_{14}–C_{21} with a 2,3,6-trimethyl substitution pattern for the aromatic ring and a tail-to-tail isoprenoid chain. They are present in very low amounts, with the C_{16} aryl isoprenoid in greatest abundance (Fig. 11). The identified aryl isoprenoids are thought to be derived from carotenoids specific for the photosynthetic green sulphur bacteria (Chlorobiaceae; Summons and Powell, 1987). These organisms are phototrophic anaerobes and thus require both light and H_2S

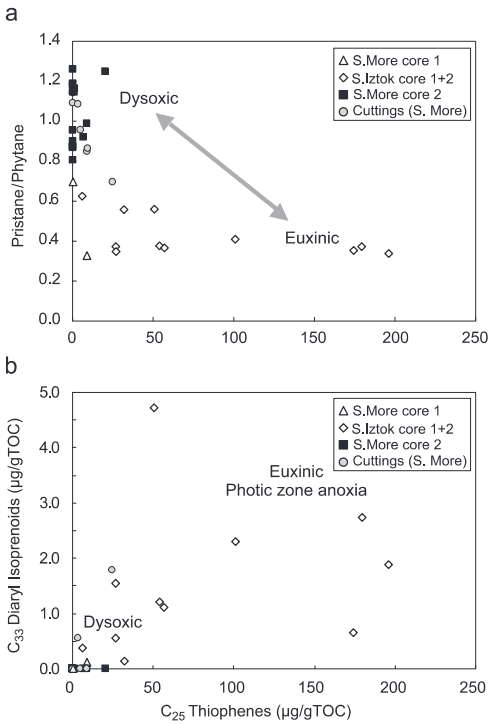

Fig. 18. (a) The pristine/phytane ratio and (b) C_{33} diaryl isoprenoids versus C_{25} thiophenes.

for growth. In modern environments they appear in sulphate-containing water bodies which a re sufficiently quiescent and organic-rich to enable sulphide production close to the photic zone (Summons, 1993). Thermal and salinity stratification is usually involved, and euxinic conditions in the deep-water zone are required (Pfennig, 1977).

However, isorenieratene itself has not been identified in the samples, so the formation of aryl isoprenoids from other precursors (i.e. b-carotene) cannot be excluded (Koopmans et al., 1996a). In the present case, higher contents of aryl isoprenoids are obtained from the samples of the Samotino More core 2 (Fig. 12). Beside the aryl isoprenoids, numerous compounds of alkyl-benzenes, methyl-alkyl-benzenes and dimethyl-alkyl-benzenes occur in these samples suggesting diagenetic conversion processes. Changes in the distribution of long-chain alkyl benzenes have been reported to co-occur with variations in the abundance and distribution of MTTCs (Sinninghe Damsté et al., 1993), reflecting salinity variations.

A C_{33} diaryl isoprenoid, undoubtedly derived from isorenieratene (Koopmans et al., 1996b), has been identified in the aromatic hydrocarbon fractions of all samples of the S. Iztok core 1 + 2 (Fig. 14), one sample of the S. More core 1, and two cutting samples at 540 and 630 m (Fig. 13). The occurrence of this compound in samples characterized by enhanced concentrations of thiophenes indicates photic zone anoxia and free H_2S in the water column (Fig. 18b).

Indications for the episodic occurrence of photic zone anoxia in shelf settings are not unusual even in facies, which are characterized as oxic/dysoxic environments. However, if anoxic conditions are prevalent, an increase in TOC and HI should be obvious. In the present case, these indications are missing. Possible explanations lie in different influencing factors on photic zone anoxia, such as water depth, water column stratification (i.e. runoff) and bioproductivity. Furthermore, dilution by mineral matter could have caused the low TOC contents of the anoxic sediments at the depositional setting.

4.6. Carbon isotopic composition of total organic carbon

The $d^{13}C$ values in the studied sections range from −27.1% to −23.7% (Table 3; Figs. 4b and 6). The results are in good agreement with the range in $d^{13}C$ obtained from the Upper Priabonian to Lower Miocene sediments of the Maykop Series in the Pericaucasus and South Caspian basins (Saint-Germès et al., 2000). The $d^{13}C$ of TOC may be influenced by the presence of free hydrocarbons of unknown origin (i.e. contamination) in the Samotino More cuttings (Fig. 10). Therefore, $d^{13}C$ of cutting samples from shallow (○ 500 m) depths must be interpreted with care. Based on the usually measured $d^{13}C$ of petroleum products and crude oils as well as on the obtained differences in SOM yields between contaminated and uncontaminated samples, contamination may result in a maximum shift of 0.5% towards lower $d^{13}C$ values. However, based on organic geochemical data, only a minor portion of cuttings samples, characterized by high PI values, show a strong contamination by a mature oil. Overall, the measured $d^{13}C$ values may reflect variable proportions of terrigenous organic carbon (~27%) versus marine organic material (~22%, Meyers, 1994). The obtained general tendency towards isotopically heavier organic carbon with increasing HI values (Fig. 19a) is in agreement with that interpretation. The total span is defined by unit V and unit VI data points, as well as by one sample of the Samotino More core 1. Only several of the samples from the Samotino More core 2 fall outside the obtained general relationship between $d^{13}C$ and HI. However, the results of several studies suggest more negative $d^{13}C$ values of marine pre-Neogene kerogens (Hertelendi and Veto, 1991; Saint-Germès et al., 2000). The more marked depletion of ^{13}C has been explained by an increase of photosynthetic carbon isotopic fractionation during periods of high concentration of atmospheric CO_2 (Popp et al., 1989), resulting in reverse carbon isotope relationship between marine and continental organic matter.

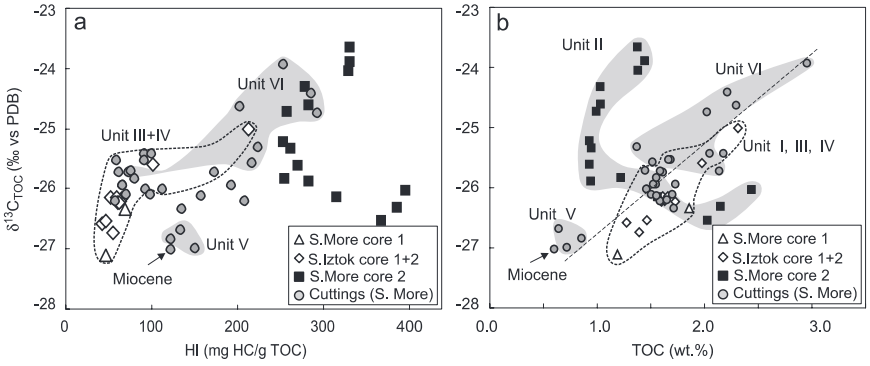

Fig. 19. Isotopic composition of organic carbon ($d^{13}C_{TOC}$) versus (a) hydrogen index (HI) and (b) total organic carbon (TOC) content.

A further positive relationship is obtained between the $d^{13}C$ values and the TOC content of most samples (Fig. 19b). Again, the Samotino More core 2 samples show a different behaviour, and the span is defined by unit V and unit VI data points. Heavier $d^{13}C$ of organic carbon with increasing TOC have been explained by CO_2 limitation and less fractionation during CO_2 uptake during periods of enhanced primary productivity (e.g. planktonic blooms; Elmore et al., 1989; Voß and Struck, 1997). Variations in $d^{13}C$ within the Ruslar Formation are therefore explained by productivity cycles and associated increased amount of autochthonous organic matter supply to the sediments.

A distinct increase in $d^{13}C$ of organic carbon with decreasing depth is observed within the Samotino More core 2 (Fig. 6). In this core, the $d^{13}C$ values are negatively correlated with carbonate content ($r^2 = 0.84$) if the lowermost samples (○ 720.2 m) are excluded. The results may indicate the effect of enhanced concentration of dissolved inorganic carbon during periods of freshwater inflow on $d^{13}C$ of organic carbon due to the intensification of the isotopic fractionation. Periods corresponding to the largest extension of anoxia, as indicated by the presence of the C_{33} diaryl isoprenoid, low pristane/phytane ratios and the occurrence of thiophenes (unit III + IV), are characterized by low $d^{13}C$ of organic matter. The results are in agreement with the data from the Maykop basin (Saint-Germès et al., 2000) suggesting an important contribution of bacterial organic matter.

4.7. Carbon and oxygen isotopic composition of calcite

The $d^{13}C$ values of the calcites vary over a relatively narrow range from −1.3% to 1.2%, and $d^{18}O$ values from −2.2% to 0.3% (Table 3; Figs. 4b and 6). The results are slightly lower in $d^{13}C$ and $d^{18}O$ as compared with the range of carbonate shells from marine molluscs of the Lower/Middle Miocene sediments of the Central Paratethys (Latal et al., 2005). Differences in the isotopic composition of calcite exist between the carbonate-rich samples of unit II (Samotino More core 2) and the rest of the sediments from the Samotino More cuttings and the Samotino Iztok core 1 + 2 (Figs. 20 and 21). The lower $d^{13}C$ and $d^{18}O$ values of calcite from unit II ("*Solenovian Event*") support the establishment of brackish conditions due to a high runoff water supply responsible for blooms of calcareous nannoplankton (Popov et al., 1993). Isotopically light $d^{18}O$ values of calcareous nannoplankton in the Toarcian Posidonia shale of SW Germany have been related to low-salinity surface waters during the monsoon-influenced summer (Röhl et al., 2001).

A negative relationship is observed between the $d^{13}C$ values of TOC and the carbon isotopic fractionation between carbonates and organic carbon ($D^{13}C_{Carb\text{-}TOC} = d^{13}C_{Carb} - d^{13}C_{TOC}$). An excellent negative correlation ($r^2 = 0.91$) exists if only the samples from the Samotino More core 2 are considered (Fig. 21). Variations in the carbon isotopic fractionation between carbonates and organic carbon are interpreted to reflect changes in surface water CO_2 concentrations (Hollander et al., 1991). Variations in the concentration of dissolved inorganic carbon (DIC) may be caused by freshwater inflow and large-scale changes in bioproductivity. The obtained negative relationships (Fig. 21) suggest that $d^{13}C$ of organic matter is mainly governed by productivity cycles. Enhanced bioproductivity results in lower carbon isotopic fractionation values ($D^{13}C_{Carb\text{-}TOC}$).

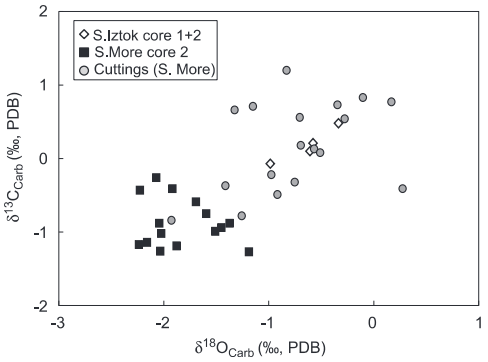

Fig. 20. Cross-correlation of $d^{13}C$ versus $d^{18}O$ of calcite.

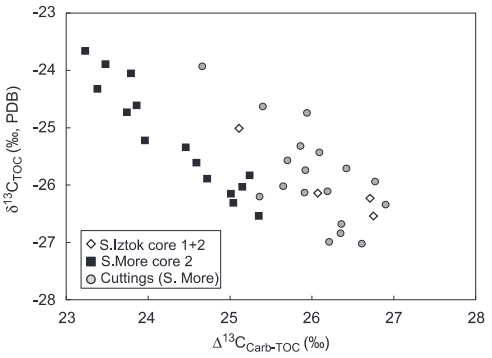

Fig. 21. Relationship between the $d^{13}C$ of organic carbon and the carbon isotopic fractionation between carbonate and organic carbon ($D^{13}C_{Carb\text{-}TOC}$).

5. Discussion

5.1. Depositional environment

Precise information on the depositional environment can be deduced from the Ruslar cores. This information is supplemented by information derived from cuttings samples. As caving is a problem in some depth intervals and as some samples are contaminated by a mature oil, the

cuttings-derived information has to be interpreted with care.

5.1.1. Redox conditions

Dysoxic to anoxic conditions prevailed during deposition of the Ruslar Formation. Within this frame, pristane/phytane ratios 4 1 indicate relatively high oxygen contents during deposition of the lower part of unit II (Samotino More core 2) and during deposition of unit VI (Figs. 13 and 14). An upward decrease in pristane/phytane ratios within Samotino More core 2 and a relatively low pristane/phytane ratio in a cuttings sample from the upper part of unit II suggest a trend towards less oxic conditions during deposition of unit II. Pristane/phytane ratios of samples from unit VI might be influenced by an oil contamination. Because the pristane/phytane ratio of the oil is low (0.64–0.78), the determined ratios (~1.1) rather underestimate than overestimate the oxygen content in unit VI.

The presence of thiophenes in samples from unit III (including core Samotino Iztok 1 + 2; Figs. 13 and 14) point to at least episodic anoxic conditions with free H_2S in the water column. This interpretation is supported by the presence of C_{33} diaryl isoprenoids, which indicates photic zone anoxia. The latter compound is also observed in unit IV. Here, however, pristane/phytane ratios indicate more oxic conditions.

5.1.2. Salinity

According to the determined di-MTTC/tri-MTTC ratios (Fig. 13), mesohaline to euhaline conditions prevailed during deposition of the Ruslar Formation. However, low di-MTTC/tri-MTTC ratios argue for brackish surface water during deposition of the lowermost part of unit II (S. More core 2). Brackish water conditions are also supported by low diversity nannoplankton assemblages dominated by *Reticulofenestra ornata* (S. More: 723–700 m depth). Based on the biomarker data, deposition of marl (~50% $calcite_{equiv}$) at about 720 m depth corresponds to a salinity minimum. Between 720 and 717 m the di-MTTC/tri-MTTC ratio increases (Fig. 14) and the $calcite_{equiv}$ percentages decrease upwards (Fig. 6). The carbonate content is mainly derived from nannoplankton. This suggests that brackish water conditions favoured nannoplankton blooms. A renewed decrease in salinity (716.8 m) had little effect on carbonate contents.

5.1.3. Organic matter input

Both, autochthonous aquatic (e.g. algae, diatoms) and allochthonous terrigenous organic material (terrestrial plants) contribute to the organic matter in the Ruslar Formation. The ratio between aquatic and terrigenous organic matter (terrestrial plants) differs significantly. According to HI values (Figs. 4 and 5) and *n*-alkanes distributions (Fig. 13), relatively high amounts of aquatic organic matter occur in the lower part of the Ruslar Formation (units I, II, lower part of unit III) and in its upper part (unit VI). Nannoplankton blooms in unit II and abundant diatoms in unit VI reflect increases in the trophic level. The presence of diatomite in unit VI also indicates input of dissolved silica. Low di-/triterpenoid ratios (Fig. 13) suggest that the terrestrial organic matter is dominated by angiosperms. Gymnosperms contribute to the organic matter mainly in units III and IV.

5.2. The "Solenovian Event" in the Western Black Sea

At the beginning of the Solenovian time (boundary between nannoplankton zones NP22/23) the Paratethys lost its connection with the World Ocean (e.g. Popov et al., 2004). High runoff water supply resulted in brackish salinities in the entire Paratethys (e.g. Budilová et al., 1992; Popov et al., 1993). Nutrients delivered into the basin by rivers caused blooms of calcareous nannoplankton adapted to the brackish water conditions. Nannoplankton blooms are recorded by light coloured marls which form a marker horizon in the Eastern Paratethys (Popov et al., 1993). Most probably dense marls overlying the manganese mineralization in the Varna District and the marls recovered by Samotino More core 2 represent this Solenovian marker horizon.

In the Alpine-Carpathian Foredeep (see Fig. 1a) time-equivalent light coloured marls are termed Dynow Marlstone (e.g., Kotlarczyk, 1979; Krhovský et al., 1991; Rusu et al., 1996; Wagner, 1998). Recently Schulz et al. (2004) studied the Dynow Marlstone in the Alpine Foredeep applying similar proxies than in the present paper. This allows a comparison of both coeval successions. Although calcite contents in the Dynow Marlstone reach up to 85%, the similarities between both successions are striking in terms of thickness (ca. 10 m) and lithology. TOC contents in both successions are controlled by the dilution of organic matter by calcareous nannoplankton and are in a similar range (Samotino More: 0.9–2.5%; Dynow Marlstone: 0.5–3.5%), but at a given carbonate content, TOC contents are generally higher in the Dynow Marlstone. Generally higher sterane/hopane ratios in the Dynow Marlstone (1.2–2.0) than in the Samotino More core 2 (0.5–1.2) suggest that this is due to higher bioproductivity in the Alpine Foredeep. Moreover, strictly anoxic conditions prevailed in the Alpine Foredeep, whereas dysoxic conditions occurred in the Kamchia Depression during early Solenovian time. Therefore, organic matter preservation was better in the Alpine Foredeep (HI: 500–600 mgHC/gTOC) than in the Kamchia Depression (HIp 400 mgHC/gTOC). Another similarity concerns a distinct upward increase in $d^{13}C$ of organic carbon in both profiles. Following the discussion in Section 4.5, this probably reflects decreasing amounts of dissolved inorganic carbon transported into the basin by surface water runoff.

5.3. Correlation between the Ruslar Formation and the Maykop Series

Only some intervals of the Ruslar Formation can be dated biostratigraphically. However, using the available

nannoplankon data together with variations in redox conditions, an approximate correlation of the Ruslar Formation with the Maykop Series in other parts of the Eastern Paratethys seems possible. Popov and Stolyarov (1996) present an overview on major Oligocene and Lower Miocene units and environmental changes in the Eastern Paratethys, which provides the background for the determination of the age of important events in the Kamchia Depression (Fig. 2).

A Late Eocene age is generally accepted for the Avren Formation and supported by the nannofossil data from the Samotino More well. However, unreleased industry data indicate that the Avren Formation continues into the Early Oligocene. Perhaps, the uppermost 40 m of the Avren Formation in the Samotino More well (810–770 m), which is devoid of nannofossils, represent the lowermost Oligocene.

A Pshekian age (NP22) is generally accepted for the manganese mineralization at the base of the Ruslar Formation in the Varna area (e.g. Popov and Stolyarov, 1996; Fig. 2). No mineralization was detected in the studied wells. However, unit I may have a similar age. Samotino More cuttings from 760 to 765 m depth yielded a NP23 age.

The bright marl at the base of unit II (NP23) is a widespread marker horizon in the Eastern Parathetys. Because of the lack of calcareous nannoplankton in the upper part of unit II and in unit III, the age of the boundary between units II and III is poorly constrained. The uppermost part of unit IV (S. More cuttings: 465–445 m depth) yielded a Late Oligocene age. A major anoxic event occurred in the Eastern Paratethys during Kalmykian time. This anoxic event is recorded in our data set in the upper part of unit III and in the lower part of unit IV (see distribution of thiophenes and C_{33} diaryl isoprenoid in Fig. 13). We, therefore, place the boundary between both units into the Kalmykian stage. Units V and VI show a return to less oxic conditions and are therefore tentatively related to the upper part of the Kalmykian stage (Fig. 2).

5.4. Hydrocarbon potential

Key parameters for the estimation of the source potential of units I–VI in different wells are shown in Table 4. The description of the hydrocarbon potential follows the classification of Peters (1986). According to TOC contents nearly all units possess a good hydrocarbon

Table 4
Summary of the source potential of different units within the Ruslar Formation in different wells

Unit	Depth (m)	Thickness (m)	Calcite equiv. (%)	TOC (%)	S2 (mgHC/gRock)	HI (mgHC/gTOC)	TOC/S
LA-IV-3							
V + VI	780–940		No samples				
IV	940–1055	115	2	1.73	3.49	196	1.25
III	1055–1100	45	0	1.55	1.96	126	1.11
II	Eroded						
I	1100–1145	45	1	1.53	2.42	156	0.89
Avren (1600–2100 m)			4	1.54	3.57	232	1.04
Samotino More							
VI	290–400	110	10	1.91	3.92	200	1.56
V	400–428	28	39	0.73	1.08	143	0.55
IV	428–590	162	4	1.58	1.38	86	0.85
III	590–665	75	3	1.51	1.07	77	0.76
II	665–725	60	8	1.48	1.56	107	0.95
I	725–770	45	4	1.71	1.93	113	0.96
Avren (770–1690 m)			20	1.00	1.47	147	0.92
Samotino Iztok							
VI	250–430		Only 1 sample				
V	430–450	20	16	1.13	1.56	133	0.76
IV	450–550	100	2	1.31	1.07	82	0.79
III	550–630	80	10	1.47	1.87	124	0.74
II	630–690	60	21	1.66	4.22	255	1.17
I	690–750	60	12	2.01	5.47	270	1.25
LA-IV-2							
VI	905–950		No samples				
V	950–980	30	25	1.54	4.29	268	1.41
IV	980–1012	32	7	1.38	1.58	114	0.63
III	1012–1037	25	18	1.37	1.99	141	0.80
II	Eroded						
I	1037–1086	49	8	1.78	4.12	232	1.00

TOC = total organic carbon, S2 = residual petroleum potential, HC = hydrocarbons, HI = hydrogen index, S = total sulphur.

potential. However, based on the S2 peak, the classification is more complex. A short summary is given below:

- *Unit I*: Unit I is characterized by average TOC contents ranging from 1.5% to 2.0%. The generative potential increases from the NW to the SE. Unit I in Samotino Iztok and LA-IV-2 have a fair to good generative potential and will generate gas and oil.
- *Unit II*: Reliable data from unit II are available from Samotino More core 2 (1.3% TOC; 304 mgHC/gTOC) and Samotino Iztok cuttings (1.7% TOC; 255 mgHC/gTOC). Based on these data, unit II has a fair generative potential and will generate gas and oil.
- *Units III/IV*: TOC contents in units III and IV are moderate (~1.5%) and HI values are generally low (77–144 mgHC/gTOC). Only unit IV in the northwestern well LA-IV-3 (1.7% TOC; 196 mgHC/gTOC) has a fair potential to generate gas and oil.
- *Unit V*: The marly unit V is relatively thin and its TOC content is low in the Samotino More (0.7%) and Samotino Iztok (1.1%) wells. However, TOC contents increase towards the southeast (LA-IV-2), where moderately high TOC contents (1.5%) and HI values (268 mgHC/gTOC) were detected. This suggests that the source potential of unit V may increase towards the deep basin.
- *Unit VI*: Data from the Samotino More well show relatively high TOC contents (1.9%) and HI values (199 mgHC/gTOC) attesting a fair generative potential for gas and oil.

The range of the analysed values from the offshore wells is in line with field data from onshore samples along the Black Sea coast (Ajdanlijsky, 2004).

As a footnote it has to be added that some intervals within the Upper Eocene Avren Formation also contain a type II–III kerogen and hold a fair generative potential for oil and gas (see well LA-IV-3 in Table 4).

6. Conclusions

The Oligocene Ruslar Formation in the Kamchia Depression offshore Bulgaria is about 450–500 m thick. It is made up predominantly of pelitic rocks with rare silt-, sand-, and limestones. Based on lithology and well logs the Ruslar Formation is subdivided from base to top into units I–VI.

Dysoxic to anoxic conditions together with meso- to euhaline salinities prevailed during deposition of the Ruslar Formation. Within this frame, relatively high oxygen contents occurred during early Solenovian times (NP23), when bright marls were deposited in a sea with reduced salinity (“*Solenovian event*”; lower part of unit II). Brackish surface water favoured nannoplankton blooms. Our results suggest an effect of enhanced concentration of dissolved inorganic carbon during periods of freshwater inflow on $\delta^{13}C$ of organic carbon due to increased isotopic fractionation.

Anoxic conditions with free H_2S in the water column and photic zone anoxia prevailed during late Oligocene times (upper part of unit III, lower part of unit IV). We speculate that these conditions reflect a basin-wide anoxic event in the Eastern Paratethys during Kalmykian times. Low $\delta^{13}C$ of organic matter indicate CO_2 recycling in a stratified water column.

Organic carbon contents in the Ruslar Formation are generally in the range of 1–2%, locally up to 3%. Autochthonous aquatic and allochthonous terrigenous biomass contribute to the organic matter. Relatively high amounts of aquatic organic matter occur in the lower part of the Ruslar Formation (units I, II, lower part of unit III) and in its upper part (unit VI). Diatoms are especially abundant in the lower part of unit VI, where biogenic silica contents reach 45%. Terrestrial organic matter is dominated by angiosperms.

The kerogen is mainly of type III, but some units contain a type II kerogen (HI 200–400 mgHC/gTOC). Using the nomenclature of Peters (1986) units I and II in the Samotino wells are characterized by a fair (locally good) potential to produce oil and gas. Units IV and V are potential sources for oil and gas in the LA wells, whereas unit VI is a fair (to good) source for oil and gas in the Samotino More well.

Acknowledgements

Technical assistance by E. Kožuharov (OMV Sofia), F. Kucher (OMV Vienna), and H.-M. Schulz (BGR Hannover) and financial support of the Austrian Science Foundation (FWF Project no. P16251-N11) to RG are gratefully acknowledged. The paper benefited greatly from the critical remarks of R. Tyson and an anonymous reviewer.

References

Abrams, M.A., Narimanov, A.A., 1996. Geochemical evaluation of hydrocarbons and their potential sources in the western South Caspian depression, Republic of Azerbaijan. Marine and Petroleum Geology 14, 451–468.

Aladžova-Hrisčeva, K., 1991. Stratigraphy, subdivision and correlation of Paleogene deposits in northeastern Bulgaria. Geologica Balkanica 21, 12–28 (in Russian).

Aleksiev, B., Bogdanova, K., 1974. The manganese deposit Obrochishte. In: Kol'kovskii, B., Dragov, P. (Eds.), Twenty Ore Deposits of Bulgaria, International Association on Genesis of Ore Deposits, IV Symposium. Geologicheskaya Rasvedka Publishers, Sofia, pp. 144–156 (in Russian).

Ajdanlijsky, G., 2004. Biostratigraphical and Source Rock Sampling of Jurassic to Miocene Successions in part of Central and Northeastern Bulgaria. GEOExplorer Ltd., Sofia, December 2004, OMV-AG In-house Report, 65pp.

Bazhenova, O.K., Fadeeva, N.P., Saint-Germes, M., Tihomirova, E.E., 2003. Deposition conditions in Western Para-Tethys ocean during the Oligocene—Early Miocene (Maykopian time). Moscow University Newspaper, Geology 6, 13–19 (in Russian).

Berner, R.A., 1984. Sedimentary pyrite formation: an update. Geochimica et Cosmochimica Acta 48, 605–615.

Bray, E.E., Evans, E.D., 1961. Distribution of *n*-paraffins as a clue to recognition of source beds. Geochimica et Cosmochimica Acta 22, 2–15.

Budilová, P., Hladíková, J., Krhovský, J., 1992. Late Eocene and Early Oligocene planktonic foraminifera and sediments of the Ždánice and Pozdrany Units: Carbon and oxygen isotopic study. Scripta 22, 67.

Ćorić, S., Zetter, R., 2004. Palynological and calcareous nannofossil biostratigraphical investigations on samples from Bulgaria, Institute of Palaeontology, University Vienna, Unpublished OMV-AG in-house report, p. 25.

Cranwell, P.A., 1977. Organic geochemistry of CamLoch (Sutherland) sediments. Chemical Geology 20, 205–221.

Dean, W.E., Arthur, M.A., 1989. Iron–sulfur–carbon relationships in organic-carbon-rich sequences, I: cretaceous western interior seaway. American Journal of Sciences 289, 708–743.

Didyk, B.M., Simoneit, B.R.T., Brassell, S.C., Eglinton, G., 1978. Organic geochemical indicators of paleoenvironmental conditions of sedimentation. Nature 272, 216–222.

Eglinton, G., Hamilton, R.J., 1967. Leaf epicuticular waxes. Science 156, 1322–1335.

Elmore, R.D., Milavec, G.J., Imbus, S.W., Engel, M.H., 1989. The Precambrian nonesuch formation of the North America Mid-Continent Rift: sedimentology and organic geochemical aspects of lacustrine deposition. Precambrian Research 43, 191–213.

Espitalié, J., LaPorte, J.L., Madec, M., Marquis, F., Leplat, P., Paulet, J., Boutefeu, A., 1977. Méthode rapide de la caractérisation des roches mères de leur potential pétrolier et de leur degré d'évolution. Revue de l'Institut Francais du Pètrole 32, 23–42.

Fadeeva, N.P., Bazhenova, O.K., 2003. Organic matter in the Maykop series from the Black—Caspian Sea region. In: 21st International meeting on Organic Geochemistry, Kraków, Poland, 8–12 September 2003, Abstracts volume.

Georgiev, G., 2000. Structure and evolution of the Western Black Sea region and Kamchiya Foredeep. Geophysical Journal 22, 91.

Georgiev, G., 2004a. Geological structure of Western Black Sea region. In: EAGE 66th Conference & Exhibition—Paris, France, 7–10 June 2004, Poster B040.

Georgiev, G.V., 1996. Hydrocarbon generation in the Tertiary filling (above the Illyrian unconformity) of the Kamchiya depression-offshore. In: Fourth International Conference "Gas in Marine Sediments," Varna, Extended Abstracts.

Georgiev, G.V., 2004. Hydrocarbon generation potential estimation in the Black Sea western zone. Sofia, June 2004, OMV-AG In-house Report.

Goossens, H., de Leeuw, J.W., Schenck, P.A., Brassell, S.C., 1984. Tocopherols as likely precursors of pristane in ancient sediments and crude oils. Nature 312, 440–442.

ten Haven, H.L., de Leeuw, J.W., Rullkötter, J., Sinninghe Damste, J.S., 1987. Restricted utility of the pristane/phytane ratio as a palaeoenvironmental indicator. Nature 330, 641–643.

ten Haven, H.L., Peakman, T.M., Rullkötter, J., 1992. Early diagenetic transformation of higher-plant triterpenoids in deep-sea sediments from Baffin Bay. Geochimica et Cosmochimica Acta 56, 2001–2024.

Hertelendi, E., Veto, I., 1991. The marine photosynthetic carbon isotopic fractionation remained constant during the early Oligocene. Palaeogeography, Palaeoclimatology, Palaeoecology 83, 333–339.

Hollander, D.J., Bessereau, G., Belin, S., Huc, A.Y., 1991. Organic matter in the Early Toarcian shales Paris Basin, France: a response to environmental changes. Revue de l'Institut Francais du Pétrole 46, 543–562.

Hussler, G., Connan, J., Albrecht, P., 1984. Novel families of tetra- and hexacyclic aromatic hopanoids predominant in carbonate rocks and crude oils. Organic Geochemistry 6, 39–49.

Karrer, W., Cherbuliez, E., Eugster, C.H., 1977. Konstitution und Vorkommen der organischen Pflanzenstoffe, Ergänzungsband I. Birkhäuser, Basel, Stuttgart, p. 1038.

Katz, B., Richards, D., Long, D., Lawrence, W., 2000. A new look at the components of the petroleum system of the South Caspian Basin. Journal of Petroleum Science and Engineering 28, 161–182.

Koopmans, M.P., Schouten, S., Kohnen, M.E.L., Sinninghe-Damsté, J.S., 1996a. Restricted utility of aryl isoprenoids as indicators for photic zone anoxia. Geochimica et Cosmochimica Acta 60, 4873–4876.

Koopmans, M.P., Köster, J., van Kaam-Peters, H.M.E., Kenig, F., Schouten, S., Hartgers, W.A., de Leeuw, J.W., Sinninghe Damsté, J.S., 1996b. Diagenetic and catagenetic products of isorenieratene: molecular indicators for photic zone anoxia. Geochimica et Cosmochimica Acta 60, 4467–4496.

Kotarba, M., Koltun, Y., 2006. Origin and habitat of hydrocarbons of the Polish and Ukrainian parts of the Carpathian Province. In: Golonka, J., Picha, F. (Eds.), The Carpathians: Geology and Hydrocarbon Resources. American Association of Petroleum Geologists Memoir, vol. 84, pp. 395–443.

Kotlarczyk, J., 1979. Introduction to stratigraphy of Skole unit of the Flysh Carpathians. Badania Paleontologiczne Karpat Przemyskich, pp. 14–26 (in Polish).

Krhovský, J., 1981. Microbiostratigraphic correlations in the Outer Flysch of the southern Moravia and influence of the eustacy on their paleogeographical development (in Czech). Zemni Plyn Nafta 26 (4), 665–688.

Krhovský, J., Adamová, M., Hladíková, J., Maslowská, H., 1991. Paleoenvironmental changes across the Eocene/Oligocene boundary in the Zdánice and Pouzdrany Units (Western Carpathians, Czechoslovakia): The long-term trend and orbitally forced changes in calcareous nannofossil assemblages. In: Hamrsmíd, B., Young, J.R. (Eds.), Nannoplankton Research. Proceedings of the Fourth International Nannoplankton Association Conference, II, Knihovnièka Zemní Plyn Nafta, vol. 14b, pp. 105–187.

LaFlamme, R.E., Hites, R.A., 1979. Tetra- and pentacyclic, naturally occurring, aromatic hydrocarbons in recent sediments. Geochimica et Cosmochimica Acta 43, 1687–1691.

Langford, F.F., Blanc-Valleron, M.-M., 1990. Interpreting Rock-Eval pyrolysis data using graphs of pyrolyzable hydrocarbons vs. total organic carbon. American Association of Petroleum Geologists Bulletin 74, 799–804.

Latal, C., Piller, W.E., Harzhauser, M., 2005. Shifts in oxygen and carbon isotope signals in marine molluscs from the Central Paratethys (Europe) around the Lower/Middle Miocene transition. Palaeogeography, Palaeoclimatology, Palaeoecology 231, 347–360.

Logan, G.A., Eglinton, G., 1994. Biogeochemistry of the Miocene lacustrine deposit at Clarkia, northern Idaho. USA Organic Geochemistry 21, 857–870.

Mackenzie, A.S., 1984. Application of biological markers in petroleum geochemistry. In: Brooks, J., Welte, D.H. (Eds.), Advances in Petroleum Geochemistry. Academic Press, London, pp. 115–214.

Mackenzie, A.S., Maxwell, J.R., 1981. Assessment of thermal maturation in sedimentary rocks by molecular measurements. In: Brooks, J. (Ed.), Organic Maturation Studies and Fossil Fuel Exploration. Academic Press, London, pp. 239–254.

Mackenzie, A.S., Hoffmann, C.F., Maxwell, J.R., 1981. Molecular parameters of maturation in the Toarcian shales, Paris Basin, France: III. Changes in aromatic steroid hydrocarbons. Geochimica et Cosmochimica Acta 45, 1345–1355.

Marinov, E., 1997. The alpine structural complex in Lower Kamchia Foredeep and the adjacent parts of East-Balkan Zone. Geology and Mineral Resources 5, 3–9.

McCrea, J.M., 1950. On the isotopic geochemistry of carbonates and palaeotemperature scale. Journal of Chemistry Physics 18, 849–857.

Meyers, P.A., 1994. Preservation of elemental and isotopic identification of sedimentary organic matter. Chemical Geology 144, 289–302.

Müller, C., 1970. Nannoplankton-Zonen der unteren Meeresmolasse Bayerns. Geologica Bavarica 63, 107–117.

Nagymarosy, A., Voronina, A.A., 1991. Calcareous nannoplankton from the Lower Maykopian Bed (Early Oligocene, Union of Independent

States). In: Proceedings of the Fourth INA Conference, 1991, pp. 189–222.
Ori, G.G., 2004. The Miocene depositional setting of northeastern Bulgaria, June 2004, unpublished OMV-AG In-house Report, p. 75.
Ourisson, G., Albrecht, P., Rohmer, M., 1979. The hopanoids: palaeochemistry and biochemistry of a group of natural products. Pure Applied Chemistry 51, 709–729.
Perch-Nielsen, K., 1984. Cenozoic calcareous nannofossils. In: Bolli, H.M., Saunders, J.B., Perch-Nielsen, K. (Eds.), Plankton Stratigraphy. Cambridge University Press, Cambridge, pp. 427–554.
Peters, K.E., 1986. Guidelines for evaluating petroleum source rock using programmed pyrolysis. American Association of Petroleum Geologists Bulletin 70, 318–329.
Pfennig, N., 1977. Phototrophic green and purple bacteria: a comparative, systematic survey. Annual Review of Microbiology 31, 275–290.
Philp, R.P., 1985. Fossil fuel biomarkers. Applications and spectra. Methods in Geochemistry and Geophysics 23, 1–294.
Popov, N., Kojumdjieva, E., 1987. The Miocene in northeastern Bulgaria (lithostratigraphic subdivision and geologic evolution). Review of the Bulgarian Geological Society 38, 15–33 (in Bulgarian).
Popov, S.V., Stolyarov, A.S., 1996. Paleogeography and anoxic environments of the Oligocene–Early Miocene Eastern Paratethys. Israel Journal of Earth Sciences 45, 161–167.
Popov, S.V., Akhmetiev, M.A., Zaporozhets, N.I., Voronina, A.A., Stolyarov, A.S., 1993. Evolution of the eastern Paratethys in the Late Eocene—Early Miocene. Stratigraphy and Geological Correlation 1, 572–600.
Popov, S.V., Rögl, F., Rozanov, A.Y., Steininger, F.F., Shcherba, I.G., Kovac, M., 2004. Lithological-Paleogeographic maps of Paratethys. 10 Maps Late Eocene to Pliocene. Courier Forschungsinstitut Senckenberg 250, 1–46.
Popp, B.N., Takigiku, R., Hayes, J.M., Louda, J.W., Baker, E.W., 1989. The post-Paleozoic chronology and mechanism of ^{13}C depletion in primary marine organic matter. American Journal of Science 289, 436–454.
Radke, M., Welte, D.H., 1983. The Methylphenanthrene Index (MPI): A maturity parameter based on aromatic hydrocarbons. In: Bjoroy, M. (Ed.), Advances in Organic Geochemistry, 1981. Wiley, Chichester, pp. 504–512.
Radke, M., Willsch, H., Welte, D.H., 1980. Preparative hydrocarbon group type determination by automated medium pressure liquid chromatography. Analytical Chemistry 52, 406–411.
Radke, M., Leythaeuser, D., Teichmüller, M., 1984. Relationship between rank and composition of aromatic hydrocarbons from coals of different origins. Organic Geochemistry 6, 423–430.
Ricken, W., 1991. Variation of sedimentation rates in rhythmically bedded sediments. Distinction between depositinal types. In: Einsele, G., Ricken, W., Seilacher, A. (Eds.), Cycles and Events in Stratigraphy. Springer, Berlin, pp. 167–187.
Robinson, A.G., Rudat, J.H., Banks, C.J., Wiles, R.L.F., 1996. Petroleum geology of the Black Sea. Marine and Petroleum Geology 13, 195–223.
Röhl, H.-J., Schmid-Röhl, A., Oschmann, W., Frimmel, A., Schwark, L., 2001. The Posidonia Shale (Lower Toarcian) of SW-Germany: an oxygen-depleted ecosystem controlled by sea level and palaeoclimate. Palaeogeography, Palaeoclimatology, Palaeoecology 165, 27–52.
Rohmer, M., Bisseret, P., Neunlist, S., 1992. The hopanoids, prokaryotic triterpenoids and precursors of ubiquitous molecular fossils. In: Moldowan, J.M., Albrecht, P., Philp, R.P. (Eds.), Biological Markers in Sediments and Petroleum. Prentice-Hall, Englewood Cliffs, NJ, pp. 1–17.
Rullkötter, J., Peakman, T.M., ten Haven, H.L., 1994. Early diagenesis of terrigenous triterpenoids and its implications for petroleum geochemistry. Organic Geochemistry 21, 215–233.
Rusu, A., Popescu, G., Melinte, M., 1996. Field Symposium Oligocene–Miocene transition and main geological events in Romania, 28 August–2 September 1996. An Excursion Guide—IGCP Project No. 326, 1–47, 21 Figs.—Bucuresti (Inst. Geol. Romaniei).
Sachsenhofer, R.F., Schulz, H.-M., 2006. Architecture of Lower Oligocene source rocks in the Alpine Foreland Basin: a model for syn- and postdepositional source rock features in the Paratethyan Realm. Petroleum Geoscience 12, 363–377.
Saint-Germès, M., Bocherens, H., Baudin, F., Bazhenova, O., 2000. Evolution of the $d^{13}C$ values of organic matter of the Maykop Series during Oligocene–Lower Miocene. Bulletin de la Société Géologique de France 171, 13–21.
Saint-Germès, M., Baudin, F., Bazhenova, O., Derenne, S., Fadeeva, N., Largeau, C., 2002. Origine et processus de la préservation de la matière organique amorphe dans la Série de Maykop (Oligocène–Miocène inférieur) du Précaucase et de l'Azerbaidjan. Bulletin de la Société Géologique de France 173, 423–436.
Schaeffer, P., Adam, P., Trendel, J.-M., Albrecht, P., Connan, J., 1995. A novel series of benzohopanes widespread in sediments. Organic Geochemistry 23, 87–89.
Schulz, H.-M., Bechtel, A., Rainer, T., Sachsenhofer, R.F., Struck, U., 2004. Palaeoceanography of the western Central Paratethys during nannoplankton zone NP 23: the Dynow Marlstone in the Austrian Molasse Basin. Geologica Carpathica 55, 311–323.
Schwark, L., Püttmann, W., 1990. Aromatic hydrocarbon composition of the Permian Kupferschiefer in the Lower Rhine Basin, N.W. Germany. Organic Geochemistry 16, 749–761.
Simoneit, B.R.T., Mazurek, M.A., 1982. Organic matter of the troposphere—II. Natural background of biogenic lipid matter in aerosols over the rural western United States. Atmospheric Environment 16, 2139–2159.
Sinclair, H.D., Juranov, S.G., Georgiev, G., Byrne, P., Mountney, N.P., 1997. The Balkan thrust wedge and foreland basin of Eastern Bulgaria: structural and stratigraphic development. In: Robinson, A.G. (Ed.), Regional and Petroleum Geology of the Black Sea and Surrounding Region. American Association of Petroleum Geologists Memoir 68, pp. 91–114.
Sinninghe Damsté, J.S., Kock-van Dalen, A.C., de Leeuw, J.W., Schenck, P.A., Guoying, S., Brassell, S.C., 1987. The identification of mono-, di-, and trimethyl 2-methyl-2-(4,8,12-trimethyltridecyl)chromans and their occurrence in the geosphere. Geochimica et Cosmochimica Acta 51, 2393–2400.
Sinninghe Damsté, J.S., van Koert, E.R., Kock-van Dalen, A.C., de Leeuw, J.W., Schenck, P.A., 1989. Characterisation of highly branched isoprenoid thiophenes occuring in sediments and immature crude oils. Organic Geochemistry 14, 555–567.
Sinninghe Damsté, J.S., Keely, B.J., Betts, S.E., Baas, M., Maxwell, J.R., de Leeuw, J.W., 1993. Variations in abundances and distributions of isoprenoid chromans and long-chain alkylbenzenes in sediments of the Mulhouse Basin: a molecular sedimentary record of palaeosalinity. Organic Geochemistry 20, 1201–1215.
Spadini, G., Robinson, A.G., Cloetingh, S.A.P.L., 1997. Thermomechanical modelling of Black Sea Basin formation, subsidence, and sedimentation. In: Robinson, A.G. (Ed.), Regional and Petroleum Geology of the Black Sea and Surrounding Region. American Association of Petroleum Geologists Memoir, 68, pp. 19–38.
Spyckerelle, C., Greiner, A.C., Albrecht, P., Ourisson, G., 1977. Aromatic hydrocarbons from geological sources. Part III. Journal of Chemical Research (M) 1977, 3746–3777.
Sukh Dev, 1989. Terpenoids. In: Rowe, J.W. (Ed.), Natural Products of Woody Plants, vol. 1. Springer, Berlin, pp. 691–807.
Summons, R.E., 1993. Biogeochemical cycles: a review of fundamental aspects of organic matter formation, preservation, and composition. In: Engel, M.H., Macko, S.A. (Eds.), Organic Geochemistry—Principles and Applications. Plenum Press, New York, pp. 3–21.
Summons, R.E., Powell, T.G., 1987. Identification of aryl isoprenoids in source rocks and crude oils: biological markers for the green sulphur bacteria. Geochimica et Cosmochimica Acta 51, 557–566.

Tiapkina, A.N., 2006. Seismic depth imaging in onshore and offshore Ukraine—case studies. In: EAGE 68th Conference & Exhibition—Vienna, Austria, 12–15 June 2006, poster P175.

Tissot, B.T., Welte, D.H., 1984. Petroleum Formation and Occurrences, second ed. Springer, Berlin, p. 699.

Trotsuk, V.Ja., Berlin, Yu.M., Marina, M.M., 1993. Petroleum generation potential offshore Bulgaria. In: Spencer, A.M. (Ed.), Generation, Accumulation and Production of Europe's Hydrocarbons III. Special Publication of the European Association of Petroleum Geoscientists, vol. 3. Springer, Berlin, pp. 325–336.

Vetö, I., 1987. An Oligocene sink for organic carbon: upwelling in the Paratethys? Palaeogeography, Palaeoclimatology, Palaeoecology 60, 143–153.

Voß, M., Struck, U., 1997. Stable nitrogen and carbon isotopes as indicators of eutrophication of the Oder River (Baltic Sea). Marine Chemistry 59, 35–49.

Volkman, J.K., 1986. A review of sterol markers for marine and terrigenous organic matter. Organic Geochemistry 9, 83–99.

Volkman, J.K., Maxwell, J.R., 1986. Acyclic isoprenoids as biological markers. In: Johns, R.B. (Ed.), Biological Markers in the Sedimentary Record. Elsevier, Amsterdam, pp. 1–42.

Wagner, L.R., 1998. Tectonostratigraphy and hydrocarbons in the Molasse Foredeep of Salz-burg, Upper and Lower Austria. In: Mascle, A., Puigdefàbregas, C., Luterbacher, H.P. (Eds.), Cenozoic Foreland Basins of Western Europe. Geological Society Special Publications, vol. 134, pp. 339–369.

Wakeham, S.G., Schaffner, C., Giger, W., 1980. Polycyclic aromatic hydrocarbons in recent lake sediments—II. Compounds derived from biological precursors during early diagenesis. Geochimica et Cosmochimica Acta 44, 415–429.

Wolff, G.A., Trendel, J.M., Albrecht, P., 1989. Novel monoaromatic triterpenoid hydrocarbons occurring in sediments. Tetrahedron 45, 6721–6728.

Zolitschka, B., 1998. Paläoklimatische Bedeutung laminierter Sedimente. Relief, Boden, Paläoklima 13, 1–176.